SANDIA REPORT

SAND2004-0872
Unlimited Release
Printed March 2004

Long Line Coupling Models

Larry K. Warne, Electromagnetics and Plasma Physics Analysis Dept.
Kenneth C. Chen, Nuclear Safety Assessment Dept.

Prepared by
Sandia National Laboratories
Albuquerque, New Mexico 87185 and Livermore, California 94550

Sandia is a multiprogram laboratory operated by Sandia Corporation,
a Lockheed Martin Company, for the United States Department of Energy's
National Nuclear Security Administration under Contract DE-AC04-94AL85000.

Approved for public release; further dissemination unlimited.

Sandia National Laboratories

Issued by Sandia National Laboratories, operated for the United States Department of Energy by Sandia Corporation.

NOTICE: This report was prepared as an account of work sponsored by an agency of the United States Government. Neither the United States Government, nor any agency thereof, nor any of their employees, nor any of their contractors, subcontractors, or their employees, make any warranty, express or implied, or assume any legal liability or responsibility for the accuracy, completeness, or usefulness of any information, apparatus, product, or process disclosed, or represent that its use would not infringe privately owned rights. Reference herein to any specific commercial product, process, or service by trade name, trademark, manufacturer, or otherwise, does not necessarily constitute or imply its endorsement, recommendation, or favoring by the United States Government, any agency thereof, or any of their contractors or subcontractors. The views and opinions expressed herein do not necessarily state or reflect those of the United States Government, any agency thereof, or any of their contractors.

Printed in the United States of America. This report has been reproduced directly from the best available copy.

Available to DOE and DOE contractors from
U.S. Department of Energy
Office of Scientific and Technical Information
P.O. Box 62
Oak Ridge, TN 37831

Telephone: (865)576-8401
Facsimile: (865)576-5728
E-Mail: reports@adonis.osti.gov
Online ordering: http://www.doe.gov/bridge

Available to the public from
U.S. Department of Commerce
National Technical Information Service
5285 Port Royal Rd
Springfield, VA 22161

Telephone: (800)553-6847
Facsimile: (703)605-6900
E-Mail: orders@ntis.fedworld.gov
Online order: http://www.ntis.gov/help/ordermethods.asp?loc=7-4-0#online

SAND2004-0872
Unlimited Release
Printed March 2004

Long Line Coupling Models

Larry K. Warne
Electromagnetics and Plasma Physics Analysis Dept.

Kenneth C. Chen
Nuclear Safety Assessment Dept.

Sandia National Laboratories
P. O. Box 5800
Albuquerque, NM 87185-1152

Abstract

This report assembles models for the response of a wire interacting with a conducting ground to an electromagnetic pulse excitation. The cases of an infinite wire above the ground as well as resting on the ground and buried beneath the ground are treated. The focus is on the characteristics and propagation of the transmission line mode. Approximations are used to simplify the description and formulas are obtained for the current. The semi-infinite case, where the short circuit current can be nearly twice that of the infinite line, is also examined.

Contents

1 INTRODUCTION **9**

2 BURIED WIRE OR INSULATED ANTENNA **9**

2.1 Complete Transmission Line Theory 10

3 WIRE ABOVE GROUND **11**

4 STATIC CALCULATIONS **13**

4.1 Insulated Filament On Ground 13

4.2 Multipole Moment Solution 14

4.2.1 multipole moments for wire above dielectric ground problem 18

4.3 Fit Function 20

5 FILAMENT WIRE ABOVE GROUND **26**

5.1 Exact Form for Evaluation of Transmission Line Parameters 26

5.2 Approximation - Complete Transmission Line Model 29

5.3 Comparison With Semi-Cylindrical Admittance 30

6 BURIED IMAGE IN GROUND PLANE **36**

7 SUMMARY OF TRANSMISSION LINE PARAMETERS **37**

8 INCIDENT PLANE WAVE **38**

8.1 Zero Frequency Limit For Numerical Transform 40

9 BELL LABS EMP WAVEFORM **43**

10 SIMULATION RESULTS **44**

10.1 Comparison of Exact Filament Current and Transmission Line Current 45

11 APPROXIMATE TRANSFORM **45**

11.1 Below Ground Case 55

11.2 Results 56

12 SEMI-INFINITE LINE **62**

13 CONCLUSIONS **64**

Figures

1. **Illustration of electric and magnetic fields surrounding insulated wire resting on nonmagnetic earth.** **12**

2. **Comparison of multipole capacitance calculation and insulated filament solution, when insulation is resting on perfect ground plane. Also shown is exact cylinder solution without insulation.** **19**

3. **Comparison of multipole capacitance calculation, fit function, and modified fit function for an insulated wire resting on a perfect ground plane. Exact cylinder solution without insulation is also shown.** **23**

4. **Comparison of capacitance multipole calculation, fit function, and modified fit function for an insulated wire slightly above a perfect ground. Exact cylinder solution without insulation is also shown.** **24**

5. **Comparison of capacitance calculation with multipole model and simple fit for an insulated wire above a perfect ground. Exact cylinder solution without insulation is also shown.** **25**

6. **Denominator function $D(k_L h)$ levels are shown for $\sigma_4 = 0.01$ S/m, $\varepsilon_{r4} = 20$, $a = 1$ cm, $h = 10$ m, and $f = 10$ MHz. Two roots are visible along with distortions arising from the two branch cuts.** **28**

7. **Comparison of normalized ground admittance for dense ground, using complete transmission line formulas and one half insulated antenna ground admittance for $(k_4/k_0)^2 = 5$.** **31**

8. **Comparison of normalized ground admittance for dense ground, using complete transmission line formulas and one half insulated antenna ground admittance for $(k_4/k_0)^2 = 10$.** **32**

9. **Comparison of normalized ground admittance for dense ground, using complete transmission line formulas and one half insulated antenna ground admittance for $(k_4/k_0)^2 = 20$.** **33**

10. **Comparison of normalized ground admittance for dense ground, using complete transmission line formulas and one half insulated antenna ground admittance for $(k_4/k_0)^2 = i20$.** **34**

11. Comparison of normalized ground admittance for dense ground, using complete transmission line formulas and one half insulated antenna ground admittance for $(k_4/k_0)^2 = i40$. 35

12. Incident angle of plane wave field. Magnetic field is taken parallel to the ground interface and perpendicular to the wire. 39

13. Transmission line model for time domain current. The blue curve is the case where the wire does not have insulation and is above ground (the incident angle was adjusted for maximum peak level, which occurs near the grazing angle). The black curve is the insulated wire (again the incident angle gives peak current). The black curve with open circles is the case where the wire is resting on the ground (again the indicent angle gives peak current, however the current in this case is insensitive to incident angle as shown by the normally incident green result). The black curve with closed circles is the buried case (normal incidence results in the maximimum current, but again the curve is insensitive to incident angle). 46

14. Comparison of exact filament result and transmission line result for the wire without insulation above ground near the grazing incidence angle. The ground conductivity in this case was $\sigma_4 = 0.01$ S/m. 47

15. Comparison of exact filament result and transmission line result for the wire without insulation above ground near the grazing incidence angle. The ground conductivity in this case was $\sigma_4 = 0.1$ S/m. 48

16. Comparison of exact filament result and transmission line result for the wire without insulation above ground near the grazing incidence angle. The ground conductivity in this case was $\sigma_4 = 0.001$ S/m. 49

17. Comparisons of Dawson integral function with simple fit functions and combination of simple fit function and asymptotic approximation. 53

18. Comparison of transmission line results with averaging approximation to inverse Laplace transform of transmission line results (dashed curves) for $\sigma_4 = 0.01$ S/m. 56

19. Comparison of transmission line results with averaging approximation to inverse Laplace transform of transmission line results (dashed curves) for $\sigma_4 = 0.1$ S/m. 57

20. Comparison of transmission line results with averaging approximation to inverse Laplace transform of transmission line results (dashed curves) for $\sigma_4 = 0.001$ S/m. 58

21. Comparison of transmission line results with averaging approximation to inverse Laplace transform of transmission line results (dashed curves) which have been shifted in time for $\sigma_4 = 0.01$ S/m. **59**

22. Comparison of transmission line results with averaging approximation to inverse Laplace transform of transmission line results (dashed curves) which have been shifted in time for $\sigma_4 = 0.1$ S/m. **60**

23. Comparison of transmission line results with averaging approximation to inverse Laplace transform of transmission line results (dashed curves) which have been shifted in time for $\sigma_4 = 0.001$ S/m. **61**

24. Comparison of transmission line results for infinite line currents (solid curves), semi-infinite short circuit currents (dashed curves), and one half the short circuit current (dot-dashed curves). The semi-infinite currents for the buried case were not plotted. **63**

25. Open circuit voltage transmission line model results. Solid curves from inverse transform. Dashed curves are short circuit current multiplied by the time averaged approximation for impedance. **64**

26. Ratio of open circuit voltage to short circuit current (solid curves) compared to time averaged characteristic impedance, which has been shifted in time by causal time shift (dashed curves). **65**

Long Line Coupling Models

1 INTRODUCTION

The purpose of this report is to provide results for the current on long conductors interacting with a conducting ground when excited by an electromagnetic pulse (EMP).

The original treatment of a wire above a conducting ground was by Carson [1] who found the formula for the ground impedance at low frequencies. Sunde [2] provided many contributions to this problem including approximations for the ground admittance and approximations for buried insulated conductors which are used in this report. Wait [3], [4] provided the exact solution of a filament above a conductive ground. Many calculations based on Wait's solution have been made including multiple wire modes, high frequency modes, and buried wires [5]. The angle of incidence which produces a maximum current has also been the subject much previous work [6], [7].

We focus on the transmission line mode of an infinite insulated wire in this report. The emphasis is on obtaining simple results for the current when the wire is either above, below, or resting on the ground. First, existing results for an insulated antenna [8], or deeply buried wire, are discussed. The complete transmission line approximation [8], which yields explicit expressions for the transmission line parameters, is reviewed and forms the basic approach in the report.

Next, an approximation for the transmission line impedance per unit length [9] is recounted and its meaning with respect to the approach of the wire to the ground is discussed.

The next few sections are concerned with obtaining the admittance per unit length, particularly as the insulated wire approaches the ground. A static solution to an insulated filament resting on the ground [10] is reviewed. This result in combination with a multipole approach are used to concoct a fit for the capacitance per unit length of an insulated wire above an electrically dense ground which is taken in series with the ground admittance. Wait's solution is examined and compared to an approximation for the ground admittance suggested by Sunde. An image is introduced to account for the transition of the buried admittance from the surface to a deeply buried situation.

The scattering solution for the filament current in terms of Wait's parameters is given (the inverse transform of this result will be compared to the transmission line result, without wire insulation, to gauge the accuracy of the transmission line model).

Next the plane wave excitation is introduced and the inverse transform is taken to obtain the current on the wire as a function of time. The Bell labs EMP waveform [11] is used for excitation. Some approximate formulas based on an averaging approximation are also given and compared to the numerical values. The semi-infinite case is also considered.

Reference works on EMP coupling to long lines along with many references can be found in [12], [13], and [14]. Corona [15], [16] and other nonlinear breakdown effects are not included in this report.

2 BURIED WIRE OR INSULATED ANTENNA

The case where the wire is buried deeply compared to the skin depth uses the transmission line model associated with the insulated antenna [8]. The current in the transmission line mode, driven by a delta

function voltage V, has the form

$$I_T = \frac{V e^{ik_L z}}{2Z_c}$$

The propagation wavenumber k_L is found from the transcendental equation [8]

$$f(k_L) = \xi_4^2 \frac{H_0^{(1)}(b\xi_4)}{b\xi_4 H_1^{(1)}(\xi_4 b)} + \frac{\mu_2 k_4^2}{\mu_4 k_2^2}\left(k_2^2 - k_L^2\right)\ln(b/a) = 0$$

$$\xi_4 = \sqrt{k_4^2 - k_L^2}$$

The characteristic impedance is

$$Z_c = \frac{-1}{4\pi\omega\varepsilon_2} f'(k_L)$$

2.1 Complete Transmission Line Theory

The most convenient approximate form is the "complete transmission line theory" with impedance per unit length [8], [12], [13]

$$Z = Z_2 + Z_4$$

$$Z_2 = -i\omega L_2$$

$$L_2 = \frac{\mu_2}{2\pi}\ln(b/a)$$

$$Z_4 = -i\omega\mu_4 H_0^{(1)}(k_4 b) / \left[2\pi k_4 b H_1^{(1)}(k_4 b)\right]$$

and admittance per unit length

$$Y = \frac{Y_2 Y_4}{Y_2 + Y_4}$$

$$Y_2 = -i\omega C_2$$

$$C_2 = 2\pi\varepsilon_2 / \ln(b/a)$$

$$Y_4 = -i2\pi(\omega\varepsilon_4 + i\sigma_4) k_4 b H_1^{(1)}(k_4 b) / H_0^{(1)}(k_4 b)$$

where the subscript 2 refers to the wire insulation properties for $a < \rho < b$ and the subscript 4 refers to the ground properties.

3 WIRE ABOVE GROUND

The case where the wire is above the ground is now considered. An approximate cylindrical model that is often used for a wire of radius b with a height h above the ground is [9]

$$Z_4 \approx -i\omega\mu_4 H_0^{(1)}(k_4 h) / \left[2\pi k_4 h H_1^{(1)}(k_4 h)\right]$$

along with the above the ground term

$$Z_0 = -i\omega\frac{\mu_0}{2\pi}\text{Arccosh}\,(h/b)$$

where

$$Z = Z_0 + Z_4$$

If we assume that all materials are nonmagnetic $\mu_2 = \mu_4 = \mu_0 = 4\pi \times 10^{-7}$ H/m it seems reasonable to take

$$Z \approx Z_0 + Z_2 + Z_4$$

where

$$Z_0 = -i\omega\frac{\mu_0}{2\pi}\text{Arccosh}\,(h/b)\ ,\ h > b$$

$$= 0\,,\ h < b$$

$$Z_2 = -i\omega\frac{\mu_0}{2\pi}\ln(b/a)$$

$$Z_4 \approx -i\omega\mu_0 H_0^{(1)}(k_4 h) / \left[2\pi k_4 h H_1^{(1)}(k_4 h)\right]\ ,\ h > b$$

$$\approx -i\omega\mu_0 H_0^{(1)}(k_4 b) / \left[2\pi k_4 b H_1^{(1)}(k_4 b)\right]\ ,\ h < b$$

It is surprising that the losses for the half space (when the wire is resting on the surface $h = b$) are the same as for the full space. However the plots in [9] appear to indicate this is indeed the case. Apparently the magnetic field on the interface extends out beyond a skin depth in such a way as to develop the same amount of loss as in the fully buried case.

The admittance is somewhat more difficult to approximate because the electric field definitely experiences discontinuities at the material boundaries as illustrated in Figure 1. Here we will simply concoct a function based on the form for the impedance. Thus we take

$$Y_4 \approx -i2\pi\left(\omega\varepsilon_4 + i\sigma_4\right) k_4 h H_1^{(1)}(k_4 h) / H_0^{(1)}(k_4 h)\ ,\ h > b$$

$$\approx -i2\pi\left(\omega\varepsilon_4 + i\sigma_4\right) k_4 b H_1^{(1)}(k_4 b) / H_0^{(1)}(k_4 b)\ ,\ h < b$$

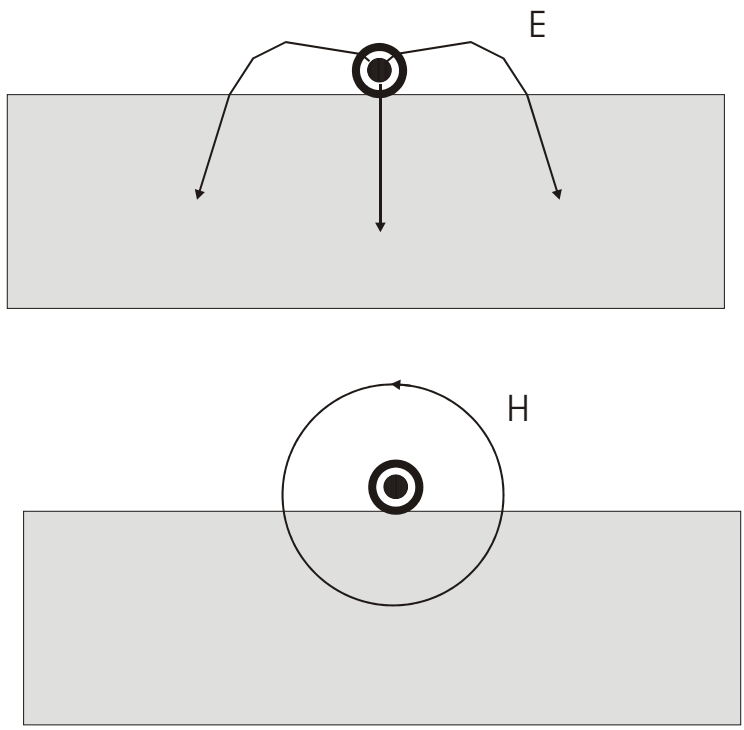

Figure 1. Illustration of electric and magnetic fields surrounding insulated wire resting on nonmagnetic earth.

$$Y_0 = \frac{-i\omega 2\pi\varepsilon_0}{\text{Arccosh}\,(h/b)}\,,\ h > b$$

$$= \infty\,,\ h < b$$

$$Y_2 = -i\omega 2\pi\varepsilon_2/\ln(b/a)$$

$$1/Y = 1/Y_0 + 1/Y_2 + 1/Y_4$$

The question is how the admittances should be modified when the wire is near the interface. This will be considered in the following sections.

4 STATIC CALCULATIONS

The static electric field is found from

$$\underline{E} = -\nabla\phi \tag{1}$$

where

$$\nabla^2\phi = -\rho/\varepsilon \tag{2}$$

The solution for a line charge q is

$$\phi = -\frac{q}{2\pi\varepsilon}\ln\left|\underline{\rho} - \underline{\rho}'\right|$$

$$= -\frac{q}{2\pi\varepsilon}\ln\sqrt{\rho^2 + \rho'^2 - 2\rho\rho'\cos(\varphi - \varphi')}$$

$$= -\frac{q}{2\pi\varepsilon}\ln\sqrt{(x - x')^2 + (y - y')^2}$$

4.1 Insulated Filament On Ground

The case of a filament resting on the ground has been solved [10]. The fields are given by (the line charge q is at the origin and the interface is at $x = b$, the radius of the cylindrical insulation)

$$E_0(z) = \frac{q}{2\pi\varepsilon_0}(1 - \Delta)\sum_{n=1}^{\infty}\Delta^{n-1}\left[\left(z - b\frac{n-1}{n}\right)^{-1} + \Delta_{04}\left(z - b\frac{n+1}{n}\right)^{-1}\right]$$

$$E_2(z) = \frac{q}{2\pi\varepsilon_2 z} + \frac{q}{2\pi\varepsilon_2}\Delta_{04}(1 - \Delta_{02})(1 - \Delta)\sum_{n=1}^{\infty}\Delta^{n-1}\left(z - b\frac{n+1}{n}\right)^{-1}$$

$$E_4(z) = \frac{q}{2\pi\varepsilon_4}(1-\Delta_{04})(1-\Delta)\sum_{n=1}^{\infty}\Delta^{n-1}\left(z - b\frac{n-1}{n}\right)^{-1}$$

where

$$E = E_x - iE_y$$

$$z = x + iy$$

$$\Delta = \Delta_{02}\Delta_{04}$$

$$\Delta_{0m} = \frac{\varepsilon_0 - \varepsilon_m}{\varepsilon_0 + \varepsilon_m}$$

If we take the half space to be perfectly conducting $\varepsilon_4 \to \infty$ and thus $\Delta_{04} \to -1$

$$E_2(z) = \frac{q}{2\pi\varepsilon_2 z} - \frac{q}{2\pi\varepsilon_2}\left(1-\Delta_{02}^2\right)\sum_{n=1}^{\infty}(-\Delta_{02})^{n-1}\left(z - b\frac{n+1}{n}\right)^{-1}$$

The potential V is now found by integrating from the small filament radius a to the interface at b

$$V = \int_a^b E_{2x}(x,0)\,dx = \frac{q}{2\pi\varepsilon_2}\ln(b/a)$$

$$+\frac{q}{2\pi\varepsilon_2}\left(1-\Delta_{02}^2\right)\sum_{n=1}^{\infty}(-\Delta_{02})^{n-1}\ln(n+1-na/b)$$

The capacitance per unit length $C = q/V$ is therefore found as

$$1/C = \frac{\ln(b/a)}{2\pi\varepsilon_2} + \frac{1}{2\pi\varepsilon_2}\left\{1 - \left(\frac{\varepsilon_{r2}-1}{\varepsilon_{r2}+1}\right)^2\right\}\sum_{n=1}^{\infty}\left(\frac{\varepsilon_{r2}-1}{\varepsilon_{r2}+1}\right)^{n-1}\ln(n+1-na/b)$$

where

$$\varepsilon_{r2} = \varepsilon_2/\varepsilon_0$$

4.2 Multipole Moment Solution

The case where the wire is near or resting on the ground is now found by use of multipole expansions. The case of a wire above ground (we take the source to be at $z = 0$ and the ground to be at $x = h$) gives real g_n and $\widehat{g}_n$

$$\phi = -\frac{q}{2\pi\varepsilon_0}\ln|z| + \sum_{n=1}^{\infty}\frac{b^n g_n}{2\pi\varepsilon_0}\operatorname{Re}(1/z^n)$$

$$+\frac{q}{2\pi\varepsilon_0}\ln|z'|-\sum_{n=1}^{\infty}\frac{(-b)^n g_n}{2\pi\varepsilon_0}\operatorname{Re}(1/z'^n)\ ,\ |z|>b$$

$$=-\frac{q^{dr}}{2\pi\varepsilon_0}\ln(b)+\sum_{n=1}^{\infty}\frac{g_n^{dr}}{2\pi\varepsilon_0 b^n}\operatorname{Re}(z^n)-\frac{\widehat{q}}{2\pi\varepsilon_0}\ln|z|+\sum_{n=1}^{\infty}\frac{b^n\widehat{g}_n}{2\pi\varepsilon_0}\operatorname{Re}(1/z^n)$$

$$+\frac{q}{2\pi\varepsilon_0}\ln|z'|-\sum_{n=1}^{\infty}\frac{(-b)^n g_n}{2\pi\varepsilon_0}\operatorname{Re}(1/z'^n)\ ,\ |z|<b$$

or

$$\phi=-\frac{q}{2\pi\varepsilon_0}\ln(\rho)+\sum_{n=1}^{\infty}\frac{(b/\rho)^n g_n}{2\pi\varepsilon_0}\cos(n\varphi)$$

$$+\frac{q}{2\pi\varepsilon_0}\ln(\rho')-\sum_{n=1}^{\infty}\frac{(-b/\rho')^n g_n}{2\pi\varepsilon_0}\cos(n\varphi')\ ,\ \rho>b$$

$$=-\frac{q^{dr}}{2\pi\varepsilon_0}\ln(b)+\sum_{n=1}^{\infty}\frac{g_n^{dr}}{2\pi\varepsilon_0(b/\rho)^n}\cos(n\varphi)-\frac{\widehat{q}}{2\pi\varepsilon_0}\ln(\rho)+\sum_{n=1}^{\infty}\frac{(b/\rho)^n\widehat{g}_n}{2\pi\varepsilon_0}\cos(n\varphi)$$

$$+\frac{q}{2\pi\varepsilon_0}\ln(\rho')-\sum_{n=1}^{\infty}\frac{(-b/\rho')^n g_n}{2\pi\varepsilon_0}\cos(n\varphi')\ ,\ \rho<b$$

where

$$z=x+iy=\rho e^{i\varphi}$$

$$-\pi<\varphi\leq\pi$$

$$z'=x-2h+iy$$

$$\rho'=\sqrt{(x-2h)^2+y^2}=\sqrt{\rho^2-4h\rho\cos\varphi+4h^2}$$

$$\varphi'=\arctan\left(\frac{y}{x-2h}\right)=\arctan\left(\frac{\rho\sin\varphi}{\rho\cos\varphi-2h}\right)$$

$$=\left[\pi-\arctan\left(\frac{\rho|\sin\varphi|}{2h-\rho\cos\varphi}\right)\right]\operatorname{sgn}(\varphi)$$

where the arctan in the final equation is taken to lie between 0 and $+\pi/2$ (if $\varphi=0$ or π we take $\varphi'=\pi$)

$$\pi/2<\varphi'\leq\pi \text{ or } -\pi<\varphi'<-\pi/2$$

Note that the potential on the ground plane is zero. Now setting the voltage equal to $\phi=V$ on $\rho=a<b$

gives

$$V=-\frac{q^{dr}}{2\pi\varepsilon_0}\ln(b)+\sum_{n=1}^{\infty}\frac{g_n^{dr}}{2\pi\varepsilon_0(b/a)^n}\cos(n\varphi)-\frac{\widehat{q}}{2\pi\varepsilon_0}\ln(a)+\sum_{n=1}^{\infty}\frac{(b/a)^n\widehat{g}_n}{2\pi\varepsilon_0}\cos(n\varphi) \tag{3}$$

$$+\frac{q}{2\pi\varepsilon_0}\ln(\rho')-\sum_{n=1}^{\infty}\frac{(-b/\rho')^n g_n}{2\pi\varepsilon_0}\cos(n\varphi')$$

where

$$\rho'=\sqrt{a^2-4ha\cos\varphi+4h^2}$$

$$\varphi'=\arctan\left(\frac{a\sin\varphi}{a\cos\varphi-2h}\right)=\left[\pi-\arctan\left(\frac{a\left|\sin\varphi\right|}{2h-a\cos\varphi}\right)\right]\operatorname{sgn}(\varphi)$$

Continuity of the potential at $\rho=b$ gives

$$-\frac{q}{2\pi\varepsilon_0}\ln(b)+\sum_{n=1}^{\infty}\frac{g_n}{2\pi\varepsilon_0}\cos(n\varphi)=-\frac{q^{dr}}{2\pi\varepsilon_0}\ln(b)+\sum_{n=1}^{\infty}\frac{g_n^{dr}}{2\pi\varepsilon_0}\cos(n\varphi)-\frac{\widehat{q}}{2\pi\varepsilon_0}\ln(b)+\sum_{n=1}^{\infty}\frac{\widehat{g}_n}{2\pi\varepsilon_0}\cos(n\varphi)$$

Because this must hold over the entire circumference we can equate the summands

$$q=q^{dr}+\widehat{q}$$

$$g_n=g_n^{dr}+\widehat{g}_n$$

Next we equate the normal component of the displacement at $\rho=b$

$$-q-\sum_{n=1}^{\infty}ng_n\cos(n\varphi)$$

$$+q\frac{b}{\rho'}\frac{\partial\rho'}{\partial\rho}+\sum_{n=1}^{\infty}n(-b/\rho')^n g_n\left[\frac{b}{\rho'}\frac{\partial\rho'}{\partial\rho}\cos(n\varphi')+b\frac{\partial\varphi'}{\partial\rho}\sin(n\varphi')\right]$$

$$=\sum_{n=1}^{\infty}n\varepsilon_{r2}g_n^{dr}\cos(n\varphi)-\varepsilon_{r2}\widehat{q}-\sum_{n=1}^{\infty}n\varepsilon_{r2}\widehat{g}_n\cos(n\varphi)$$

$$+q\varepsilon_{r2}\frac{b}{\rho'}\frac{\partial\rho'}{\partial\rho}+\sum_{n=1}^{\infty}n(-b/\rho')^n g_n\varepsilon_{r2}\left[\frac{b}{\rho'}\frac{\partial\rho'}{\partial\rho}\cos(n\varphi')+b\frac{\partial\varphi'}{\partial\rho}\sin(n\varphi')\right] \tag{4}$$

where

$$\frac{\partial\rho'}{\partial\rho}=(\rho-2h\cos\varphi)/\sqrt{\rho^2-4h\rho\cos\varphi+4h^2}$$

$$\frac{\partial \varphi'}{\partial \rho} = \frac{-2h \sin \varphi}{\rho^2 - 4h\rho \cos \varphi + 4h^2}$$

and on $\rho = b$

$$\rho' = \sqrt{b^2 - 4hb \cos \varphi + 4h^2}$$

$$\varphi' = \arctan\left(\frac{b \sin \varphi}{b \cos \varphi - 2h}\right) = \left[\pi - \arctan\left(\frac{b\,|\sin \varphi|}{2h - b \cos \varphi}\right)\right] \operatorname{sgn}(\varphi)$$

$$\frac{\partial \rho'}{\partial \rho} = (b - 2h \cos \varphi) / \sqrt{b^2 - 4hb \cos \varphi + 4h^2}$$

$$b\frac{\partial \varphi'}{\partial \rho} = \frac{-2hb \sin \varphi}{b^2 - 4hb \cos \varphi + 4h^2}$$

$$\frac{b}{\rho'}\frac{\partial \rho'}{\partial \rho} = \frac{b\,(b - 2h \cos \varphi)}{b^2 - 4hb \cos \varphi + 4h^2}$$

If we truncate the series at $n = N$ we have $2N + 2$ unknowns (q^{dr}, q, g_n, and g_n^{dr}). The constant V is set and $\widehat{q}$ and $\widehat{g}_n$ are related by the above equations. If we match (3) and (4) at the points

$$\varphi = m\pi/N \ , \ m = 0, 1, ..., N$$

we then have $2N + 2$ equations in $2N + 2$ unknowns. The capacitance per unit length is found from

$$C = q/V$$

Thus we can take $V = 1$ and the capacitance per unit length is the charge per unit length.

$$2\pi\varepsilon_0 V = q \ln(\rho'/a) - q^{dr} \ln(b/a)$$

$$+ \sum_{n=1}^{\infty} g_n \left\{(b/a)^n \cos(n\varphi) - (-b/\rho')^n \cos(n\varphi')\right\} + \sum_{n=1}^{\infty} \left\{(a/b)^n - (b/a)^n\right\} g_n^{dr} \cos(n\varphi)$$

where

$$\rho' = \sqrt{a^2 - 4ha \cos \varphi + 4h^2}$$

$$\varphi' = \left[\pi - \arctan\left(\frac{a\,|\sin \varphi|}{2h - a \cos \varphi}\right)\right] \operatorname{sgn}(\varphi)$$

$$q = q^{dr} + \widehat{q}$$

$$g_n = g_n^{dr} + \widehat{g}_n$$

$$0 = q\left(1-\varepsilon_{r2}\right) - \left(1-\varepsilon_{r2}\right) q \frac{b}{\rho'} \frac{\partial \rho'}{\partial \rho}$$

$$+\sum_{n=1}^{\infty} n\left(1-\varepsilon_{r2}\right) g_n \cos\left(n\varphi\right) - \sum_{n=1}^{\infty} n\left(1-\varepsilon_{r2}\right)\left(-b/\rho'\right)^n g_n \left[\frac{b}{\rho'}\frac{\partial \rho'}{\partial \rho}\cos\left(n\varphi'\right) + b\frac{\partial \varphi'}{\partial \rho}\sin\left(n\varphi'\right)\right]$$

$$+\varepsilon_{r2} q^{dr} + \sum_{n=1}^{\infty} 2n\varepsilon_{r2} g_n^{dr} \cos\left(n\varphi\right)$$

where

$$\frac{\partial \rho'}{\partial \rho} = \left(\rho - 2h\cos\varphi\right) / \sqrt{\rho^2 - 4h\rho\cos\varphi + 4h^2}$$

$$\frac{\partial \varphi'}{\partial \rho} = \frac{-2h\sin\varphi}{\rho^2 - 4h\rho\cos\varphi + 4h^2}$$

and on $\rho = b$

$$\rho' = \sqrt{b^2 - 4hb\cos\varphi + 4h^2}$$

$$\varphi' = \left[\pi - \arctan\left(\frac{b\left|\sin\varphi\right|}{2h - b\cos\varphi}\right)\right] \operatorname{sgn}\left(\varphi\right)$$

$$\frac{\partial \rho'}{\partial \rho} = \left(b - h\cos\varphi\right) / \sqrt{b^2 - 2hb\cos\varphi + 4h^2}$$

$$b\frac{\partial \varphi'}{\partial \rho} = \frac{-2hb\sin\varphi}{b^2 - 4hb\cos\varphi + 4h^2}$$

$$\frac{b}{\rho'}\frac{\partial \rho'}{\partial \rho} = \frac{b\left(b - 2h\cos\varphi\right)}{b^2 - 4hb\cos\varphi + 4h^2}$$

Figure 2 shows a comparison of the multipole model, the filament model [10], and the formula (for $\varepsilon_{r2} = 1$)

$$C/\varepsilon_0 = 2\pi/\mathrm{Arccosh}\left(h/a\right)$$

4.2.1 multipole moments for wire above dielectric ground problem

We replace the reflection coefficient of minus one by the reflection coefficient of the dielectric boundary

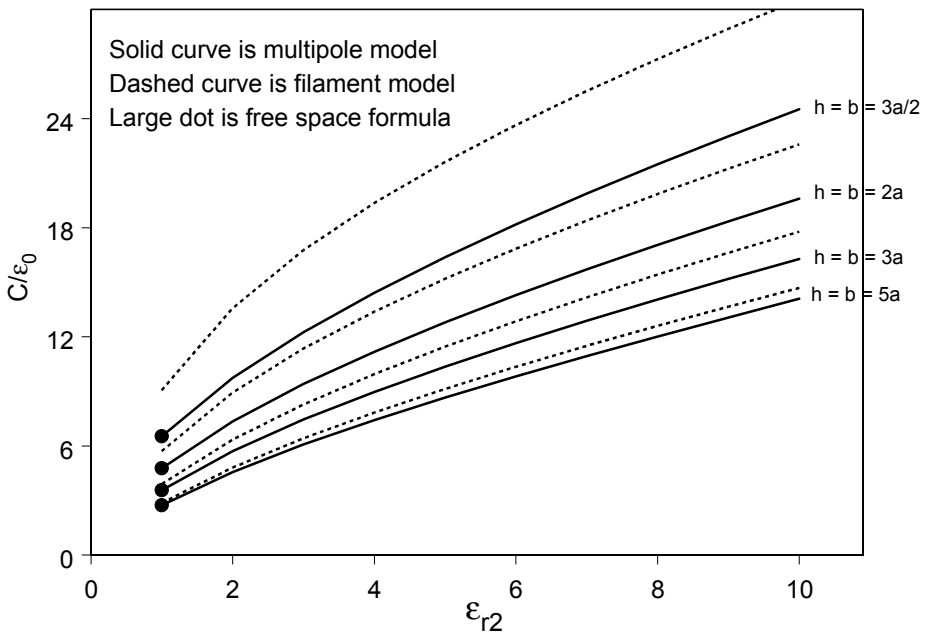

Figure 2. Comparison of multipole capacitance calculation and insulated filament solution, when insulation is resting on perfect ground plane. Also shown is exact cylinder solution without insulation.

$$\phi = -\frac{q}{2\pi\varepsilon_0}\ln(\rho) + \sum_{n=1}^{\infty}\frac{(b/\rho)^n g_n}{2\pi\varepsilon_0}\cos(n\varphi)$$

$$+\frac{\varepsilon_4-\varepsilon_0}{\varepsilon_4+\varepsilon_0}\left[\frac{q}{2\pi\varepsilon_0}\ln(\rho') - \sum_{n=1}^{\infty}\frac{(-b/\rho')^n g_n}{2\pi\varepsilon_0}\cos(n\varphi')\right],\ \rho > b$$

$$= -\frac{q^{dr}}{2\pi\varepsilon_0}\ln(b) + \sum_{n=1}^{\infty}\frac{g_n^{dr}}{2\pi\varepsilon_0(b/\rho)^n}\cos(n\varphi) - \frac{\widehat{q}}{2\pi\varepsilon_0}\ln(\rho) + \sum_{n=1}^{\infty}\frac{(b/\rho)^n\widehat{g}_n}{2\pi\varepsilon_0}\cos(n\varphi)$$

$$+\frac{\varepsilon_4-\varepsilon_0}{\varepsilon_4+\varepsilon_0}\left[\frac{q}{2\pi\varepsilon_0}\ln(\rho') - \sum_{n=1}^{\infty}\frac{(-b/\rho')^n g_n}{2\pi\varepsilon_0}\cos(n\varphi')\right],\ \rho < b$$

If the conductivity is important $\varepsilon_4 \to \varepsilon_4 + i\sigma_4/\omega$.

4.3 Fit Function

What if we took the fit for the wire resting on the ground (with relatively thin insulation) to be

$$\phi = -\frac{q_0}{2\pi\varepsilon_0}\left[\ln\sqrt{(x-h_e)^2+y^2} - \ln\sqrt{(x+h_e)^2+y^2}\right]$$

$$h_e = \sqrt{h^2-b^2}$$

where the potential vanishes on the the ground plane. On the insulation, $x-h = b\cos\varphi$ and $y = b\sin\varphi$, we find potential

$$\phi = V_0 = \frac{q_0}{2\pi\varepsilon_0}\ln\left(\frac{h+h_e}{b}\right) = q_0/C_0$$

or

$$C_0 = \frac{2\pi\varepsilon_0}{\mathrm{Arccosh}(h/b)}$$

and charge density (here we take $x = h+\rho\cos\varphi$ and $y = \rho\sin\varphi$)

$$D_\rho = \varepsilon_0 E_\rho = -\varepsilon_0\frac{\partial\phi}{\partial\rho}$$

$$= \frac{q_0 h_e/(2\pi b)}{h+b\cos\varphi}\ ,\ q_0 = C_0 V_0$$

We take the electric field in the thin layer to be

$$E_\rho \approx \frac{b}{\rho}D_\rho(b)/\varepsilon_2$$

then the voltage drop in the layer is

$$V - V_0(\varphi) \approx \frac{2\pi b}{C_2} D_\rho(b)$$

where

$$C_2 = \frac{2\pi\varepsilon_2}{\ln(b/a)}$$

Inserting the zero order charge density

$$D_\rho(b) \approx \frac{C_0 V_0 h_e / (2\pi b)}{h + b\cos\varphi}$$

gives the first order voltage

$$V_0(\varphi) \approx \frac{V(h + b\cos\varphi)}{h + b\cos\varphi + h_e C_0/C_2}$$

and then the first order charge density

$$D_\rho(b) \approx \frac{V C_0 h_e / (2\pi b)}{(h + h_e C_0/C_2) + b\cos\varphi}$$

Using the identity [17]

$$\frac{1}{\pi}\int_0^\pi \frac{d\varphi}{1 + A\cos\varphi} = \frac{1}{\sqrt{1 - A^2}}$$

gives the first order charge

$$q = CV = 2\int_0^\pi D_\rho b d\varphi = \frac{V C_0 h_e}{\sqrt{(h + h_e C_0/C_2)^2 - b^2}}$$

Thus the first order capacitance is

$$1/C \approx \sqrt{\left(\frac{h/h_e}{C_0} + \frac{1}{C_2}\right)^2 - \left(\frac{b/h_e}{C_0}\right)^2}$$

When $h = b$ this becomes

$$C \approx C_2/\sqrt{1 + C_2/(\pi\varepsilon_0)}$$

When $h >> b$ this becomes

$$1/C \approx 1/C_2 + 1/C_0$$

To improve the fit we allow the relation between the voltage drop in the layer and the charge density to have one asymmetrical mode

$$V - V_0(\varphi) \approx \frac{2\pi b}{C_2} D_\rho(b)(1 + A_2\cos\varphi)$$

$$\approx \frac{V_0 h_e C_0/C_2}{h + b\cos\varphi}\left(1 + A_2\cos\varphi\right)$$

or

$$V_0\left(\varphi\right) \approx \frac{V\left(h + b\cos\varphi\right)}{\left(h + h_e C_0/C_2\right) + \left(b + h_e A_2 C_0/C_2\right)\cos\varphi}$$

The modified fit is then

$$1/C \approx \sqrt{\left(\frac{h/h_e}{C_0} + \frac{1}{C_2}\right)^2 - \left(\frac{b/h_e}{C_0} + \frac{A_2}{C_2}\right)^2}$$

where we take

$$A_2 = 0.7\left(1 - a/b\right)\frac{\varepsilon_2 - \varepsilon_0}{\varepsilon_2 + \varepsilon_0}\left(1 - h_e/h\right)$$

With this fit function we take as an approximation to the total admittance

$$1/Y \approx 1/\left(-i\omega C\right) + 1/Y_4$$

When the lower half space is electrically dense the second term is small. When $h = b$ this capacitance becomes

$$C \approx C_2/\sqrt{\left(1 - A_2\right)\left\{1 + A_2 + C_2/\left(\pi\varepsilon_0\right)\right\}}$$

$$A_2 = 0.7\left(1 - a/b\right)\frac{\varepsilon_2 - \varepsilon_0}{\varepsilon_2 + \varepsilon_0}$$

When $h >> b$ this capacitance again becomes

$$1/C \approx 1/C_2 + 1/C_0$$

This modified fit allows the wire to continuously approach the interface. The presence of the constant A_2 accounts for the leading term of asymmetry in the localized capacitance relation between the charge density and voltage on the insulation surface.

A comparison of the multipole solution, and this fit function are shown in Figure 3 for a wire with insulation resting on a perfectly conducting (or very electrically dense) ground. Figure 4 shows this comparison when the insulation is just slightly above the perfectly conducting ground.

When the cable is not resting on the ground the simple fit can be taken as that proposed originally

$$C \approx 1/C_2 + 1/C_0$$

Figure 5 shows this fit when the cable center height is twice the insulation radius.

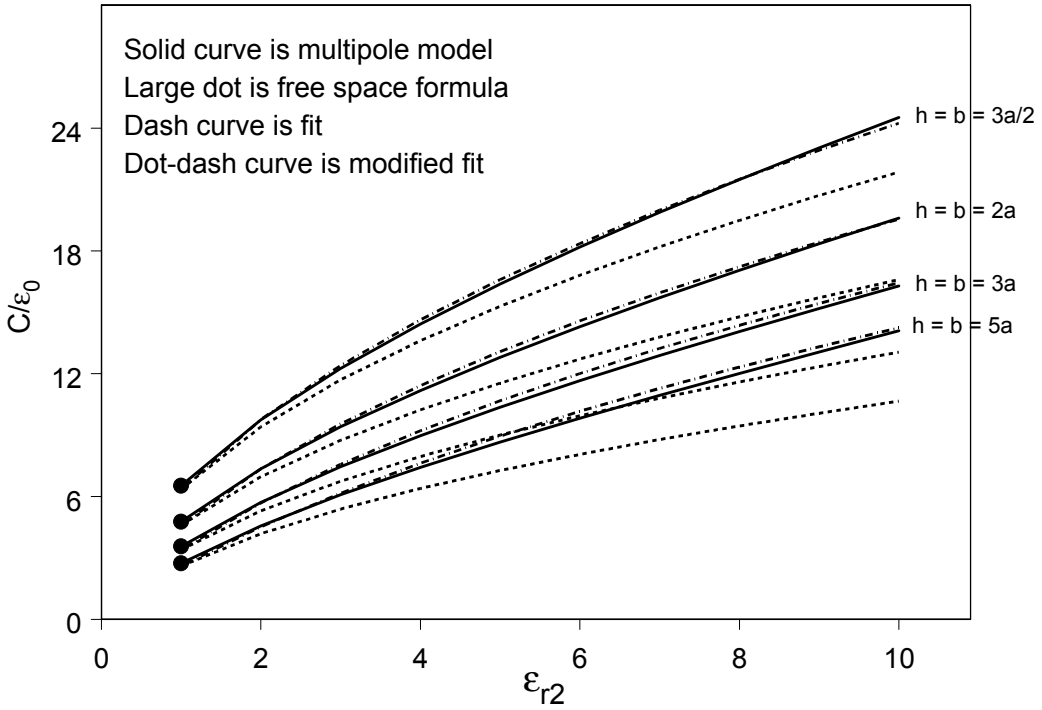

Figure 3. Comparison of multipole capacitance calculation, fit function, and modified fit function for an insulated wire resting on a perfect ground plane. Exact cylinder solution without insulation is also shown.

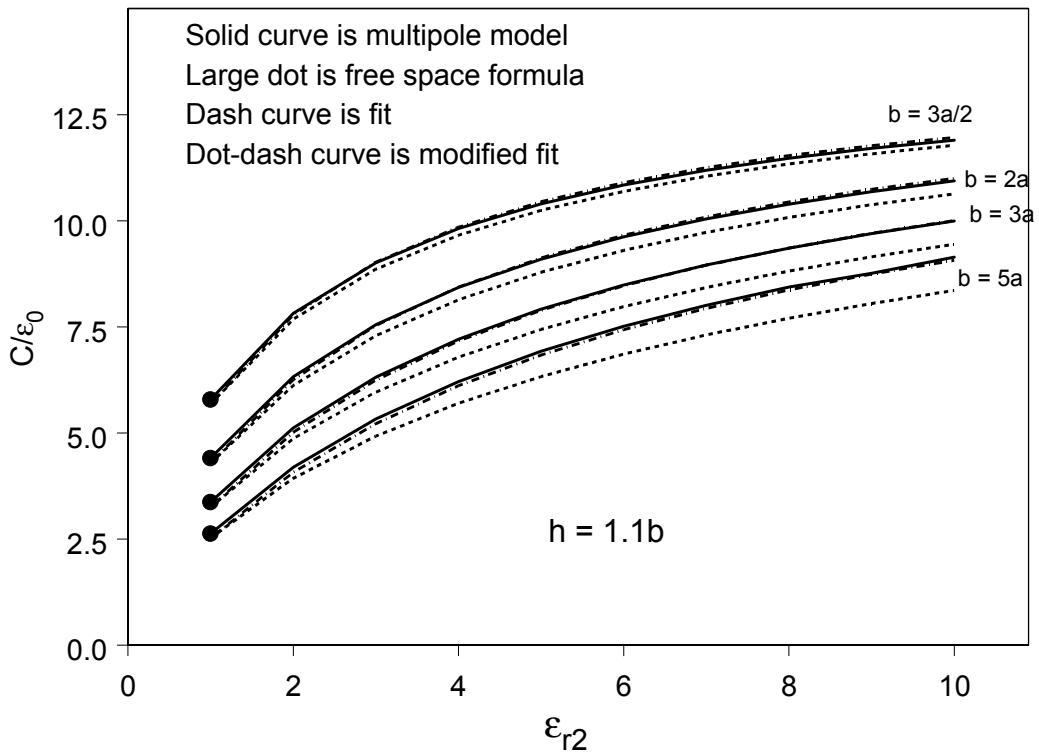

Figure 4. Comparison of capacitance multipole calculation, fit function, and modified fit function for an insulated wire slightly above a perfect ground. Exact cylinder solution without insulation is also shown.

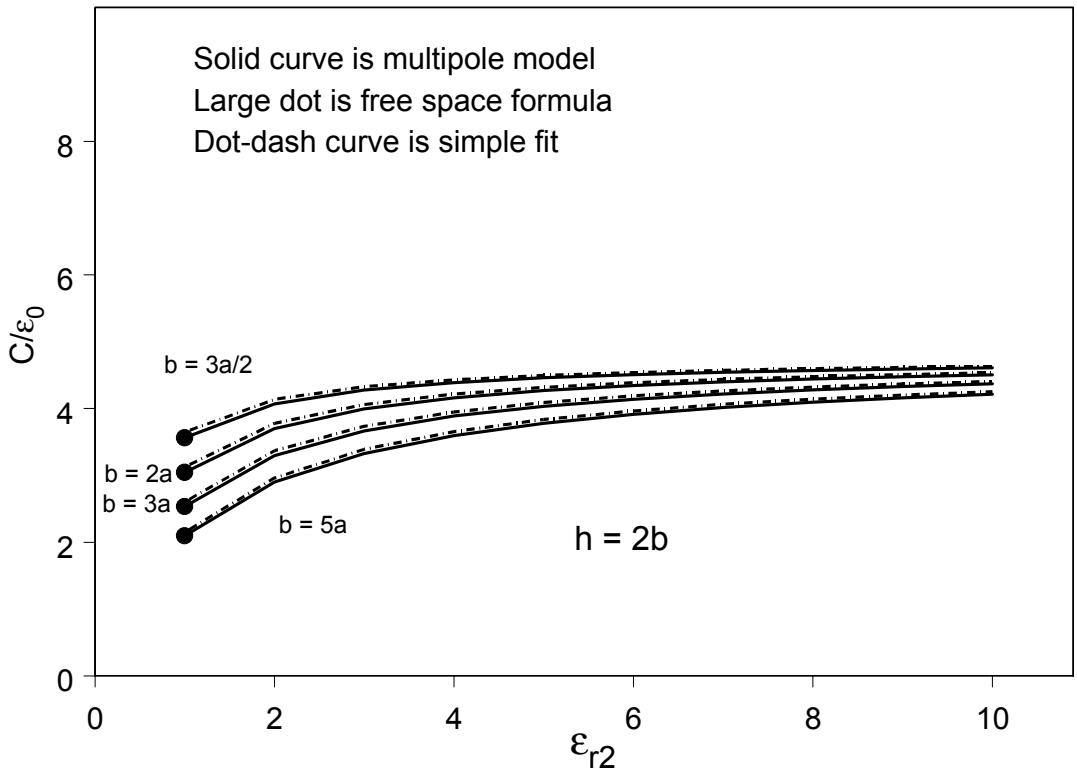

Figure 5. Comparison of capacitance calculation with multipole model and simple fit for an insulated wire above a perfect ground. Exact cylinder solution without insulation is also shown.

5 FILAMENT WIRE ABOVE GROUND

It is instructive to examine the known solution of a filament above ground [3], [4].

5.1 Exact Form for Evaluation of Transmission Line Parameters

The forms used are

$$Z = -i\omega \frac{\mu_0}{2\pi} \left[\Lambda + 2\left(Q + iP\right)\right]$$

$$Y = -i\omega 2\pi\varepsilon_0 / \left[\Lambda + 2\left(N + iM\right)\right]$$

$$\Lambda = K_0\left[-ia\sqrt{k_0^2 - k_L^2}\right] - K_0\left[-i\sqrt{k_0^2 - k_L^2}\sqrt{4h^2 + a^2}\right]$$

$$K_0\left(-iz\right) = i\frac{\pi}{2}H_0^{(1)}\left(z\right)\ ,\ -\frac{\pi}{2} < \arg\left(z\right) \leq \pi$$

$$\mathrm{Im}\sqrt{k_0^2 - k_L^2} \geq 0$$

$$Q + iP = \int_0^\infty e^{-u_0 2h}\cos\left(\lambda a\right)\frac{d\lambda}{u_0 + u_4}$$

$$N + iM = \int_0^\infty e^{-u_0 2h}\cos\left(\lambda a\right)\frac{d\lambda}{\left(k_4/k_0\right)^2 u_0 + u_4}$$

$$u_0 = \sqrt{\lambda^2 + k_L^2 - k_0^2} = -i\sqrt{k_0^2 - k_L^2 - \lambda^2}$$

$$\mathrm{Im}\sqrt{k_0^2 - k_L^2 - \lambda^2} \geq 0$$

$$u_4 = \sqrt{\lambda^2 + k_L^2 - k_4^2} = -i\sqrt{k_4^2 - k_L^2 - \lambda^2}$$

$$\mathrm{Im}\sqrt{k_4^2 - k_L^2 - \lambda^2} \geq 0$$

$$k_0^2 = \omega^2\mu_0\varepsilon_0$$

$$k_4^2 = \omega^2\mu_0\left(\varepsilon_4 + i\sigma_4/\omega\right)$$

$$-ik_L = \sqrt{ZY}$$

Note that we replace ε_4 by $\varepsilon_4 + i\sigma_4/\omega$ to introduce the conductivity.

Let us define a "residue" characteristic impedance [3]

$$Z_c^R = \frac{V}{2I_t} = -\frac{\omega\mu_0}{4\pi}\frac{\partial D(k_L)}{\partial k_L}$$

where

$$D(k_L) = \left(1 - k_L^2/k_0^2\right)\left[K_0\left\{-ia\sqrt{k_0^2 - k_L^2}\right\} - K_0\left\{-i\sqrt{4h^2 + a^2}\sqrt{k_0^2 - k_L^2}\right\}\right]$$

$$+2\int_0^\infty \left[\frac{1}{u_0 + u_4} - \frac{k_L^2}{k_0^2 u_4 + k_4^2 u_0}\right] e^{-2u_0 h}\cos(\lambda a)\, d\lambda$$

or

$$\left(\frac{-i\omega\mu_0}{2\pi}\right) D = Z + k_L^2/Y$$

and

$$\frac{\partial D(k_L)}{\partial k_L} = \left(-2k_L/k_0^2\right)\left[K_0\left\{-ia\sqrt{k_0^2 - k_L^2}\right\} - K_0\left\{-i\sqrt{4h^2 + a^2}\sqrt{k_0^2 - k_L^2}\right\}\right]$$

$$+\frac{k_L}{k_0^2}\sqrt{k_0^2 - k_L^2}\left[-iaK_1\left\{-ia\sqrt{k_0^2 - k_L^2}\right\} + i\sqrt{4h^2 + a^2}K_1\left\{-i\sqrt{4h^2 + a^2}\sqrt{k_0^2 - k_L^2}\right\}\right]$$

$$-4k_L\int_0^\infty \frac{1}{k_0^2 u_4 + k_4^2 u_0} e^{-2u_0 h}\cos(\lambda a)\, d\lambda$$

$$-2k_L\int_0^\infty \left[\frac{1}{u_0 + u_4} - k_L^2\frac{\left(k_0^2 u_0 + k_4^2 u_4\right)}{\left(k_0^2 u_4 + k_4^2 u_0\right)^2}\right] e^{-2u_0 h}\cos(\lambda a)\frac{d\lambda}{u_0 u_4}$$

The propagation constant is found from

$$D(k_L) = 0$$

Rigorous treatments of this equation lead to a fairly complicated set of solutions [5] with two pole contributions (Figure 6 shows these roots of $D(k_L h)$ for $h = 10$ m, $f = 10$ MHz, $\varepsilon_{r4} = 20$, and $\sigma_4 = 0.01$ S/m). It is known that the transmission line approximation yields currents which are near the exact integral transform solution [18], [19]. Approximations to the transcendental equation such as setting $k_L \to k_0$ in $Z(k_L)$ and in $Y(k_L)$ have been used to simplify the results and generalize the original Carson treatment of the problem when the wire is above the ground [4]. In the next section we introduce something similar to this approximation but we further take the wire height and insulation radius to be electrically small.

Note that the electric field resulting from the filamentary wire current can be written as

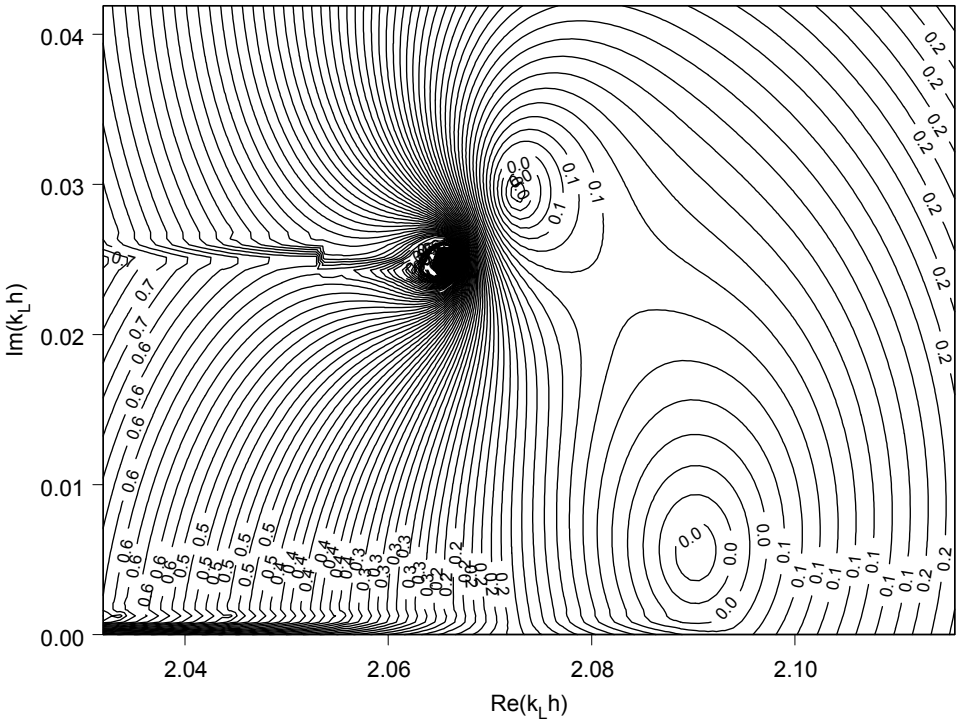

Figure 6. Denominator function $D(k_L h)$ levels are shown for $\sigma_4 = 0.01$ S/m, $\varepsilon_{r4} = 20$, $a = 1$ cm, $h = 10$ m, and $f = 10$ MHz. Two roots are visible along with distortions arising from the two branch cuts.

$$E_z = -\frac{B\left(k_0 \cos\theta_0\right)}{D\left(k_0 \cos\theta_0\right)} E_z^{inc}$$

where [3], [4]

$$B\left(k_L\right) = \left(1 - k_L^2/k_0^2\right)\left[K_0\left\{-i\sqrt{\left(x-h\right)^2 + y^2}\sqrt{k_0^2 - k_L^2}\right\} - K_0\left\{-i\sqrt{\left(x+h\right)^2 + y^2}\sqrt{k_0^2 - k_L^2}\right\}\right]$$

$$+2\int_0^\infty \left[\frac{1}{u_0 + u_4} - \frac{k_L^2}{k_0^2 u_4 + k_4^2 u_0}\right] e^{-u_0(x+h)} \cos\left(\lambda y\right) d\lambda$$

and E_z^{inc} is the field incident at the wire center without the wire present (it includes the reflection from the ground plane). An impedance boundary condition can be used here if it is desired to add an internal impedance per unit length for the wire [4]. Noting that the Hertz potential along the wire can be found from this as $\Pi_z = E_z / \left(k_0^2 - k_L^2\right)$, and that the singular part of the azimuthal magnetic field about the wire can be found as the curl of this axial Hertz potential, we find the wire current as the integral of the magnetic field around the wire [4]

$$I = \frac{E_z^{inc}}{-i\omega\mu_0 D\left(k_0 \cos\theta_0\right) / \left(2\pi\right)}$$

This exact form of the filament current will be inverse transformed and compared with the transmission line solutions.

5.2 Approximation - Complete Transmission Line Model

We take the half space to be electrically dense $|k_4| >> |k_L|, k_0$ and consider the upper half space as static, such that $k_0 h$, $k_L h$, $k_0 a$, and $k_L a \to 0$. Then we have

$$Z = -i\omega\frac{\mu_0}{2\pi}\left[\Lambda + 2\left(Q + iP\right)\right]$$

$$Y = -i\omega 2\pi\varepsilon_0 / \left[\Lambda + 2\left(N + iM\right)\right]$$

$$\Lambda \approx \ln\sqrt{4h^2/a^2 + 1}$$

$$Q + iP \approx \int_0^\infty e^{-\lambda 2h} \cos\left(\lambda a\right) \frac{d\lambda}{\lambda + u_4}$$

$$N + iM \approx \int_0^\infty e^{-\lambda 2h} \cos\left(\lambda a\right) \frac{d\lambda}{\left(k_4/k_0\right)^2 \lambda + u_4}$$

$$u_4 \approx \sqrt{\lambda^2 - k_4^2}$$

The wavenumber is

$$-ik_L = \sqrt{ZY}$$

Applying the derivative to these approximate forms gives the characteristic impedance as

$$Z_c = -\frac{\omega\mu_0}{4\pi}\frac{\partial D\left(k_L\right)}{\partial k_L} \approx -ik_L/Y$$

Thus the transmission line parameters then approximately become

$$Z \approx -i\omega\frac{\mu_0}{2\pi}\left[\ln\sqrt{4h^2/a^2+1} + 2\int_0^\infty e^{-\lambda 2h}\cos\left(\lambda a\right)\frac{d\lambda}{\lambda+\sqrt{\lambda^2-k_4^2}}\right]$$

$$\approx -i\omega\frac{\mu_0}{2\pi}\left[\ln\sqrt{4h^2/a^2+1} + \frac{2}{k_4^2}\int_0^\infty e^{-\lambda 2h}\cos\left(\lambda a\right)\left(\lambda-\sqrt{\lambda^2-k_4^2}\right)d\lambda\right]$$

$$Y \approx -i\omega 2\pi\varepsilon_0/\left[\ln\sqrt{4h^2/a^2+1} + 2\int_0^\infty e^{-\lambda 2h}\cos\left(\lambda a\right)\frac{d\lambda}{\left(\varepsilon_4/\varepsilon_0\right)\lambda+\sqrt{\lambda^2-k_4^2}}\right]$$

5.3 Comparison With Semi-Cylindrical Admittance

Let us drop a compared to h, but replace the logarithm by the PEC solution

$$Z \approx -i\omega\frac{\mu_0}{2\pi}\left[\mathrm{Arccosh}\left(h/a\right) + \frac{2}{k_4^2}\int_0^\infty e^{-\lambda 2h}\left(\lambda-\sqrt{\lambda^2-k_4^2}\right)d\lambda\right]$$

$$Y \approx -i\omega 2\pi\varepsilon_0/\left[\mathrm{Arccosh}\left(h/a\right) + 2\int_0^\infty e^{-\lambda 2h}\frac{d\lambda}{\left(\varepsilon_4/\varepsilon_0\right)\lambda+\sqrt{\lambda^2-k_4^2}}\right]$$

where the impedance is Carson's result [1]. Let us define

$$-i\omega 2\pi\varepsilon_0/Y_4 = 2\int_0^\infty e^{-u}\frac{du}{\left(k_4/k_0\right)^2 u+\sqrt{u^2-4k_4^2h^2}}$$

We compare this with twice the insulated antenna formula [2] (Sunde indicates that this is a reasonable approximation. It is the admittance to a semi-cylinder.)

$$-i\omega 4\pi\varepsilon_0/Y_4 \approx 2\frac{H_0^{(1)}\left(k_4h\right)}{\left(k_4/k_0\right)^2 k_4hH_1^{(1)}\left(k_4h\right)}$$

Figures 7, 8, and 9 show comparisons for real k_4 (low conductivity). This approximation seems to work fairly well when $k_4h < 0.5$.

Figures 10 and 11 show comparisons for 45° k_4 (high conductivity). The relative agreement is not as good in these cases, however, the conductivity must be fairly high in these case to dominate over the permittivity and thus the contribution from the Y_4 tends to decrease relative to the wire insulation contribution.

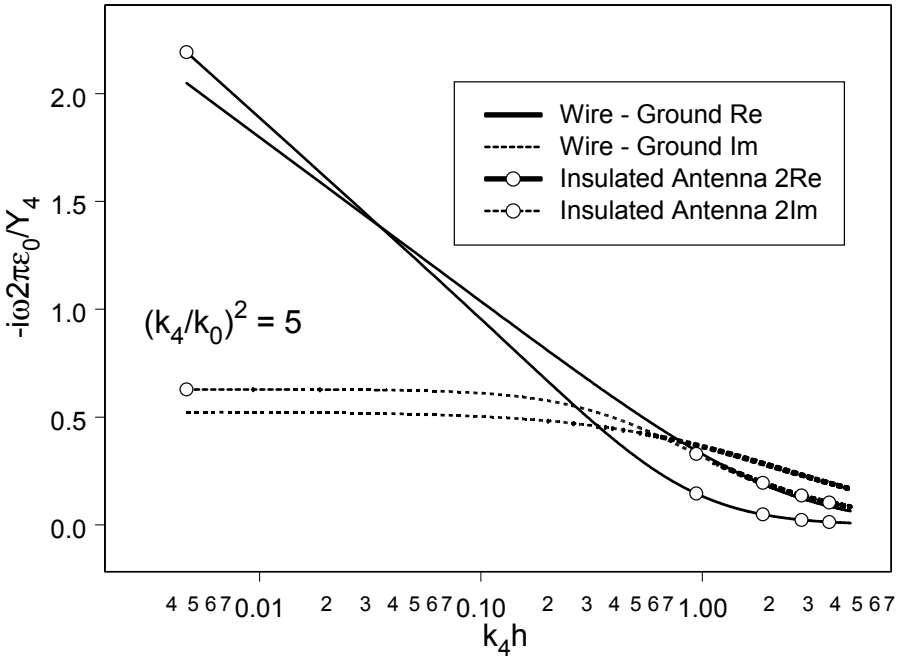

Figure 7. Comparison of normalized ground admittance for dense ground, using complete transmission line formulas and one half insulated antenna ground admittance for $(k_4/k_0)^2 = 5$.

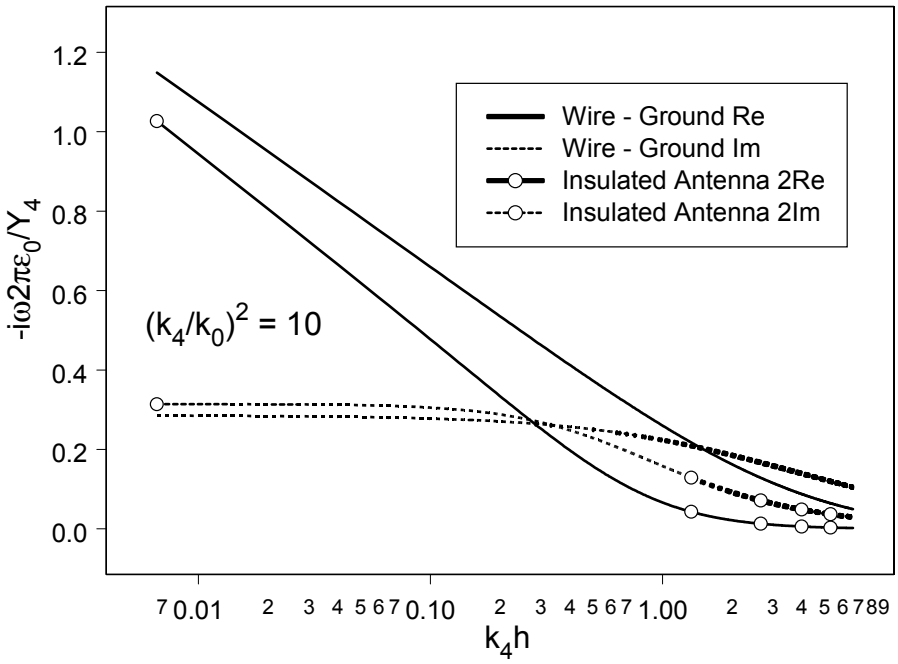

Figure 8. Comparison of normalized ground admittance for dense ground, using complete transmission line formulas and one half insulated antenna ground admittance for $(k_4/k_0)^2 = 10$.

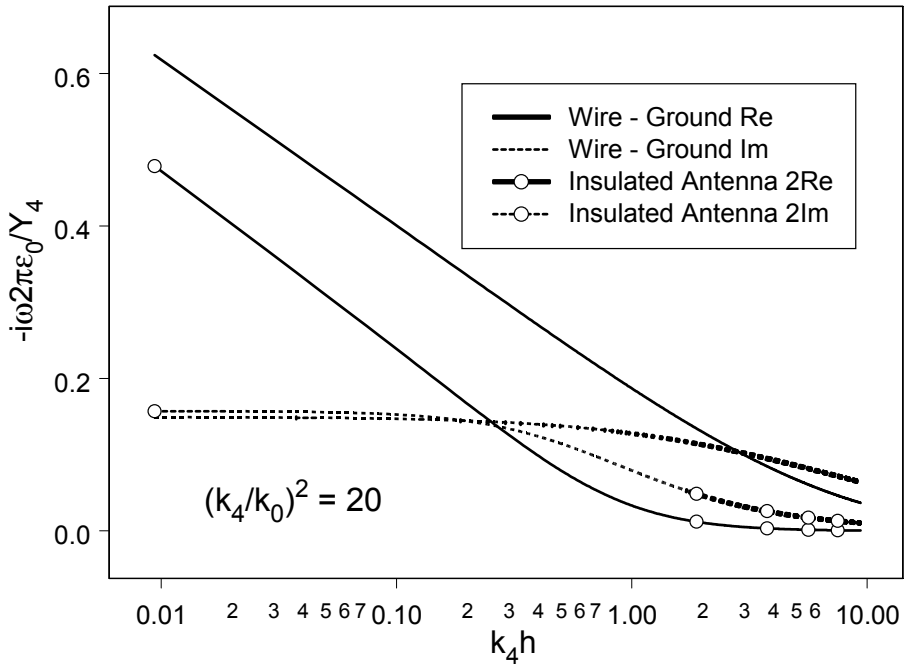

Figure 9. Comparison of normalized ground admittance for dense ground, using complete transmission line formulas and one half insulated antenna ground admittance for $(k_4/k_0)^2 = 20$.

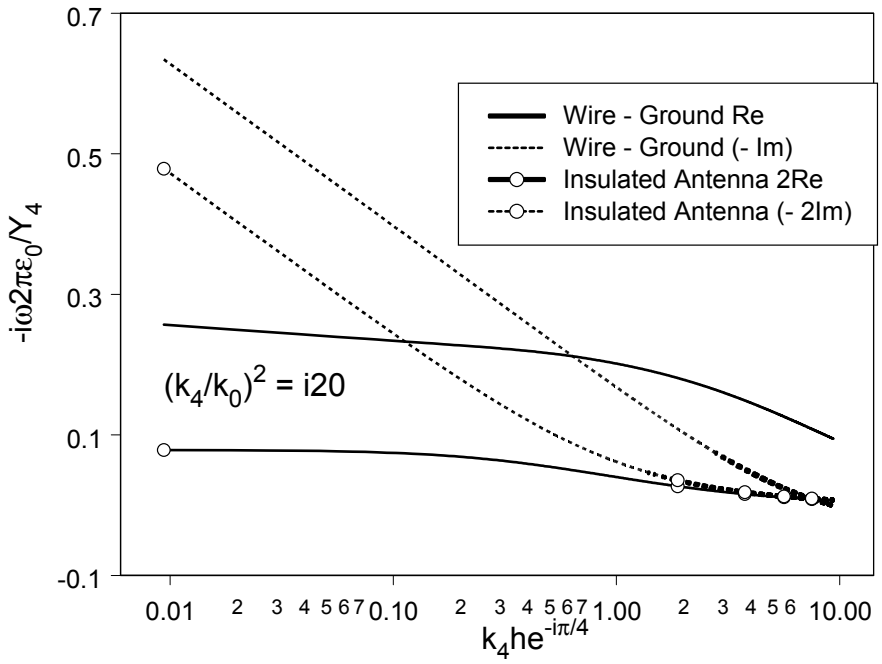

Figure 10. Comparison of normalized ground admittance for dense ground, using complete transmission line formulas and one half insulated antenna ground admittance for $(k_4/k_0)^2 = i20$.

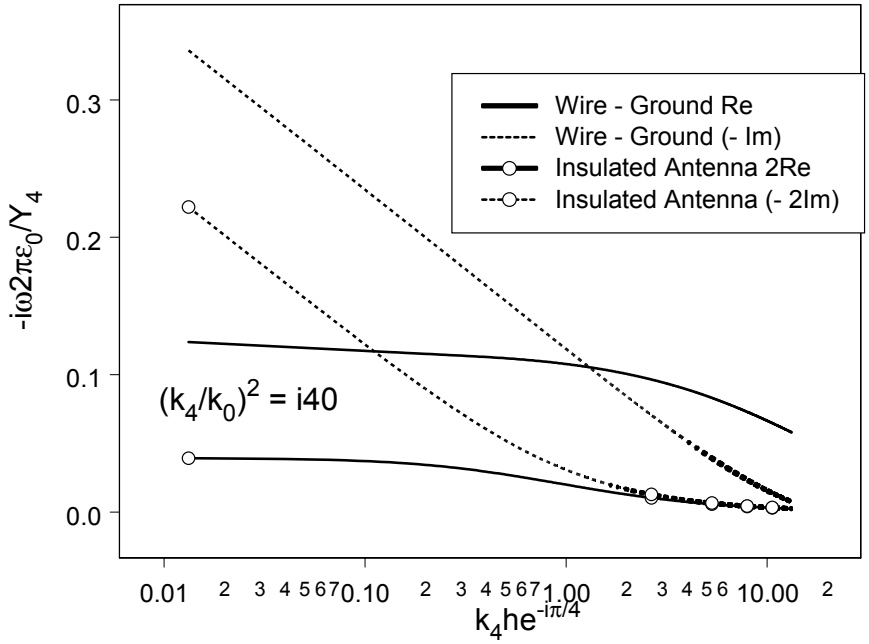

Figure 11. Comparison of normalized ground admittance for dense ground, using complete transmission line formulas and one half insulated antenna ground admittance for $(k_4/k_0)^2 = i40$.

6 BURIED IMAGE IN GROUND PLANE

Because Sunde's suggestion of taking half the ground admittance seems to work (at least when the ground permittivity was dominant) we now consider how the insulated antenna makes the transition as it approaches the ground plane. Treating the ground as electrically dense we can take the approximate boundary condition as

$$E_x\left(x=0\right)\approx 0$$

Adding an image to the primary potential of the current filament gives the potential as the solution of

$$\left(\nabla^2+k_4^2\right)A_z=-\mu_0 J_z$$

or with $h<0$

$$A_z\approx\frac{i}{4}\mu_0 I e^{ik_L z}\left[H_0^{(1)}\left(\xi_4\sqrt{\left(x+h\right)^2+y^2}\right)+H_0^{(1)}\left(\xi_4\sqrt{\left(x-h\right)^2+y^2}\right)\right]\ ,\ x<0$$

$$\approx\frac{i}{4}\mu_0 I e^{ik_L z}\left[H_0^{(1)}\left(k_4\sqrt{\left(x+h\right)^2+y^2}\right)+H_0^{(1)}\left(k_4\sqrt{\left(x-h\right)^2+y^2}\right)\right]\ ,\ x<0$$

where we have ignored k_L compared to k_4. The scalar potential is

$$i\mu_0\left(\omega\varepsilon_4+i\sigma_4\right)\phi=\frac{\partial A_z}{\partial z}=ik_L A_z$$

The transverse field is then

$$\underline{E}_t=-\nabla_t\phi$$

The voltage on the insulation can thus be taken as

$$V=\phi\left(h,b\right)$$

$$\approx\frac{i}{4}\mu_0 I e^{ik_L z}\left[H_0^{(1)}\left(k_4 b\right)+H_0^{(1)}\left(k_4\sqrt{4h^2+b^2}\right)\right]$$

The current leaving the insulation is (here we take $x=h+\rho\cos\varphi$ and $y=\rho\sin\varphi$)

$$I_t=\int_0^{2\pi}\left(\sigma_4-i\omega\varepsilon_4\right)E_\rho b d\varphi$$

$$\approx\frac{i}{4}\mu_0 I e^{ik_L z}\left(\sigma_4-i\omega\varepsilon_4\right)2\pi k_4 b H_1^{(1)}\left(k_4 b\right)$$

The admittance per unit length is thus

$$Y_4=I_t/V\approx -i\omega 2\pi\left(\varepsilon_4+i\sigma_4/\omega\right)k_4 b H_1^{(1)}\left(k_4 b\right)/\left[H_0^{(1)}\left(k_4 b\right)+H_0^{(1)}\left(k_4\sqrt{4h^2+b^2}\right)\right]$$

Thus when $h\to 0$ we end up with half the admittance just as Sunde suggested. This formula gives an estimate for the transition as the wire approaches the interface from below; the important parameter is $2k_4 h$.

7 SUMMARY OF TRANSMISSION LINE PARAMETERS

The summary of the above investigation is now assembled. The impedance is found by means of

$$Z = Z_0 + Z_2 + Z_4$$

where

$$Z_0 = -i\omega \frac{\mu_0}{2\pi} \text{Arccosh}\left(h/b\right) \ , \ h \geq b$$

$$= 0 \, , \, h < b$$

$$Z_2 = -i\omega \frac{\mu_0}{2\pi} \ln\left(b/a\right)$$

$$Z_4 \approx -i\omega\mu_0 H_0^{(1)}\left(k_4 h\right) / \left[2\pi k_4 h H_1^{(1)}\left(k_4 h\right)\right] \ , \ h \geq b$$

$$\approx -i\omega\mu_0 H_0^{(1)}\left(k_4 b\right) / \left[2\pi k_4 b H_1^{(1)}\left(k_4 b\right)\right] \ , \ h < b$$

$$k_4^2 = \omega\mu_0\left(\omega\varepsilon_4 + i\sigma_4\right)$$

and the admittance is found by means of

$$1/Y = 1/Y_e + 1/Y_4$$

$$Y_e = -i\omega C_e$$

$$1/C_e \approx \sqrt{\left(\frac{h/h_e}{C_0} + \frac{1}{C_2}\right)^2 - \left(\frac{b/h_e}{C_0} + \frac{A_2}{C_2}\right)^2} \ , \ h \geq b$$

$$\approx 1/C_2 \ , \ h < -b$$

$$A_2 = 0.7\left(1 - a/b\right)\frac{\varepsilon_2 - \varepsilon_0}{\varepsilon_2 + \varepsilon_0}\left(1 - h_e/h\right)$$

$$h_e = \sqrt{h^2 - b^2}$$

$$C_0 = \frac{2\pi\varepsilon_0}{\text{Arccosh}\left(h/b\right)} \, , \, h \geq b$$

$$C_2 = 2\pi\varepsilon_2 / \ln\left(b/a\right)$$

$$Y_4 \approx -i\pi\left(\omega\varepsilon_4 + i\sigma_4\right) k_4 h H_1^{(1)}\left(k_4 h\right) / H_0^{(1)}\left(k_4 h\right) \ , \ h \geq b$$

$$\approx -i2\pi\left(\omega\varepsilon_4 + i\sigma_4\right) k_4 b H_1^{(1)}\left(k_4 b\right) / \left[H_0^{(1)}\left(k_4 b\right) + H_0^{(1)}\left(k_4\sqrt{4h^2+b^2}\right)\right] \ , \ h < -b$$

The admittance in the range of incomplete burial $-b \leq h < b$ is not considered here.

8 INCIDENT PLANE WAVE

The coupling to the transmission line mode from an incident plane wave is now considered. This is the same calculation as carried out previously [6], [7]. The transmission line equations are

$$\frac{dV}{dz} = -ZI + E_z^{inc}$$

$$\frac{dI}{dz} = -YV$$

Eliminating the voltage gives

$$\left(\frac{d^2}{dz^2} + k_L^2\right) I = -YE_z^{inc}$$

Let us take the incident plane wave to be polarized in the plane containing the wire and the ground surface with incidence angle θ_0 with respect to the z axis as shown in Figure 12. Thus the incident magnetic field is

$$H_y^{inc} = \frac{1}{\eta_0} E\left(\omega\right)\left[e^{izk_0\cos\theta_0 - ixk_0\sin\theta_0} + R_H e^{izk_0\cos\theta_0 + ixk_0\sin\theta_0}\right] \ , \ x > 0$$

$$H_y^{inc} = \frac{1}{\eta_0} E\left(\omega\right) T_H e^{izk_0\cos\theta_0 - ix\sqrt{k_4^2 - k_0^2\cos^2\theta_0}} \ , \ x < 0$$

where R_H is the reflection coefficient from the interface and T_H is the transmission coefficient. Matching continuity of tangential electric and magnetic field components gives [20]

$$E_z^{inc} = \frac{1}{-i\omega\varepsilon_0}\frac{H_y^{inc}}{\partial x} = E\left(\omega\right)\sin\theta_0\left[e^{izk_0\cos\theta_0 - ixk_0\sin\theta_0} - R_H e^{izk_0\cos\theta_0 + ixk_0\sin\theta_0}\right]$$

$$E_z^{inc} = \frac{1}{-i\left(\omega\varepsilon_4 + i\sigma_4\right)}\frac{H_y^{inc}}{\partial x} = \frac{\sqrt{\left(k_4/k_0\right)^2 - \cos^2\theta_0}}{\left(k_4/k_0\right)^2} E\left(\omega\right) T_H e^{izk_0\cos\theta_0 - ix\sqrt{k_4^2 - k_0^2\cos^2\theta_0}}$$

and

$$1 + R_H = T_H$$

$$1 - R_H = \frac{\sqrt{\left(k_4/k_0\right)^2 - \cos^2\theta_0}}{\left(k_4/k_0\right)^2\sin\theta_0} T_H$$

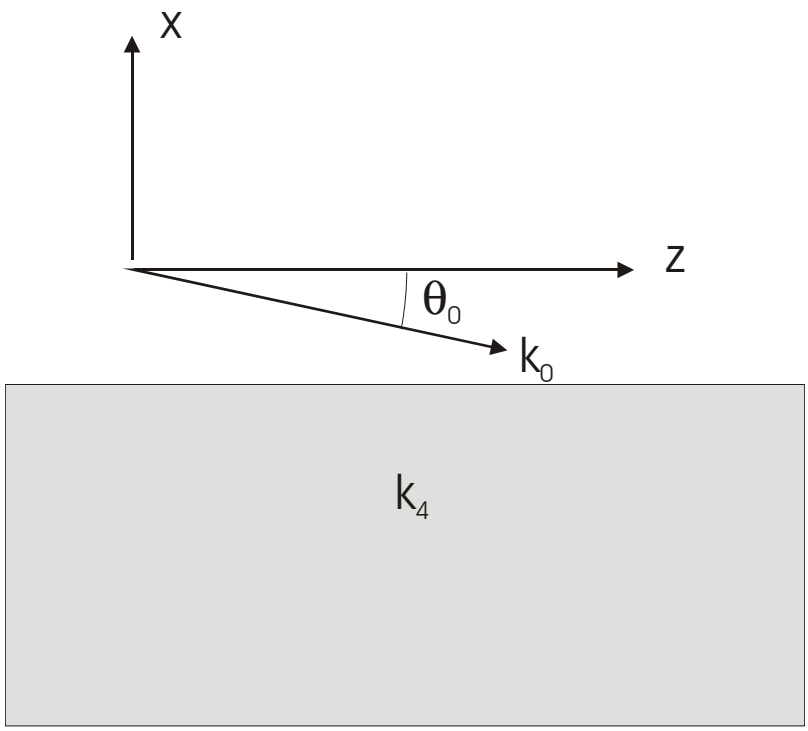

Figure 12. Incident angle of plane wave field. Magnetic field is taken parallel to the ground interface and perpendicular to the wire.

Adding yields

$$T_H = \frac{2\left(k_4/k_0\right)^2 \sin\theta_0}{\left(k_4/k_0\right)^2 \sin\theta_0 + \sqrt{\left(k_4/k_0\right)^2 - \cos^2\theta_0}}$$

and

$$R_H = \frac{\left(k_4/k_0\right)^2 \sin\theta_0 - \sqrt{\left(k_4/k_0\right)^2 - \cos^2\theta_0}}{\left(k_4/k_0\right)^2 \sin\theta_0 + \sqrt{\left(k_4/k_0\right)^2 - \cos^2\theta_0}}$$

When $h > 0$ we have the field along the wire

$$E_z^{inc} = E\left(\omega\right)\sin\theta_0\left[e^{-ihk_0\sin\theta_0} - R_H e^{ihk_0\sin\theta_0}\right]e^{izk_0\cos\theta_0} = A_0 e^{izk_0\cos\theta_0}$$

When $h < 0$ we have the field along the wire

$$E_z^{inc} = E\left(\omega\right)\frac{\sqrt{\left(k_4/k_0\right)^2 - \cos^2\theta_0}}{\left(k_4/k_0\right)^2} T_H e^{izk_0\cos\theta_0 - ih\sqrt{k_4^2 - k_0^2\cos^2\theta_0}} = A_4 e^{izk_0\cos\theta_0}$$

The general solution of the transmission line equation

$$\left(\frac{d^2}{dz^2}+k_L^2\right)I=-YA_ne^{izk_0\cos\theta_0}$$

is found as homogeneous plus particular solutions

$$I=c_1e^{ik_Lz}+c_2e^{-ik_Lz}-\frac{YA_ne^{izk_0\cos\theta_0}}{k_L^2-k_0^2\cos^2\theta_0}$$

For the infinite wire we drop the homogeneous terms (since these would blow up at $\pm\infty$)

$$I=-\frac{YA_ne^{izk_0\cos\theta_0}}{k_L^2-k_0^2\cos^2\theta_0}$$

8.1 Zero Frequency Limit For Numerical Transform

The limit $\omega\to 0$ is now examined since it is more convenient to handle the low frequency piece of the transform integrals separately. The expansions are

$$k_4\sim\sqrt{i\omega\mu_0\sigma_4}=(1+i)\sqrt{\omega\mu_0\sigma_4/2}=(1+i)/\delta_4$$

$$(k_4/k_0)\sim\sqrt{i\sigma_4/(\omega\varepsilon_0)}$$

$$\delta_4=\sqrt{2/(\omega\mu_0\sigma_4)}$$

$$Y=\frac{Y_eY_4}{Y_e+Y_4}$$

$$Y_e=-i\omega C_e$$

$$Y_4\sim -i2\sigma_4/\left[1+i\frac{2}{\pi}\left\{\ln\left(\frac{1}{2}k_4h\right)+\gamma\right\}\right]\ ,\ h\geq b$$

$$Y_4\sim -i2\sigma_4/\left[1+i\frac{2}{\pi}\left\{\ln\left(\frac{1}{2}k_4b\right)+\gamma\right\}\right]\ ,\ h<-b$$

$$Y\sim -i\omega C_e$$

$$Z=Z_e+Z_4$$

$$Z_e=-i\omega\frac{\mu_0}{2\pi}\left\{\ln(b/a)+\mathrm{Arccosh}\,(h/b)\right\}\ ,\ h\geq b$$

$$=-i\omega\frac{\mu_0}{2\pi}\ln(b/a)\ ,\ h<b$$

$$= -i\omega\frac{\mu_0}{2\pi}\ln\left(2h_{eff}/a\right)$$

$$Z_4 \sim \frac{1}{4}\omega\mu_0\left[1 + i\frac{2}{\pi}\left\{\ln\left(\frac{1}{2}k_4 h\right) + \gamma\right\}\right]\ ,\ h \geq b$$

$$\sim \frac{1}{4}\omega\mu_0 i\frac{2}{\pi}\left\{\ln\left(\frac{1}{2}k_4 h\right) + \gamma - i\frac{\pi}{2}\right\}\ ,\ h \geq b$$

$$\sim i\omega\mu_0\frac{\mu_0}{2\pi}\ln\left(\frac{1}{2}e^{\gamma}h\sqrt{-i\omega\mu_0\sigma_4}\right)\ ,\ h \geq b$$

$$\sim i\omega\mu_0\frac{\mu_0}{2\pi}\ln\left(\frac{1}{2}e^{\gamma}b\sqrt{-i\omega\mu_0\sigma_4}\right)\ ,\ h < b$$

$$Z \sim -i\omega\frac{\mu_0}{2\pi}\ln\left(\frac{4h_{eff}}{e^{\gamma}ha\sqrt{-i\omega\mu_0\sigma_4}}\right)\ ,\ h \geq b$$

$$\sim -i\omega\frac{\mu_0}{2\pi}\ln\left(\frac{4h_{eff}}{e^{\gamma}ba\sqrt{-i\omega\mu_0\sigma_4}}\right)\ ,\ h < b$$

$$k_L^2 = -ZY \sim \omega^2 C_e\frac{\mu_0}{2\pi}\ln\left(\frac{4h_{eff}}{e^{\gamma}ha\sqrt{-i\omega\mu_0\sigma_4}}\right)\ ,\ h \geq b$$

$$\sim \omega^2 C_e\frac{\mu_0}{2\pi}\ln\left(\frac{4h_{eff}}{e^{\gamma}ba\sqrt{-i\omega\mu_0\sigma_4}}\right)\ ,\ h < b$$

$$R_H \sim \frac{(k_4/k_0)\sin\theta_0 - 1}{(k_4/k_0)\sin\theta_0 + 1}$$

$$\sim 1 - \frac{2}{(k_4/k_0)\sin\theta_0 + 1}$$

$$\sim 1 - 2\sqrt{\omega\varepsilon_0/\left(i\sigma_4\right)}\csc\theta_0$$

$$T_H \sim \frac{2\left(k_4/k_0\right)\sin\theta_0}{(k_4/k_0)\sin\theta_0 + 1}$$

$$\sim 2 - \frac{2}{(k_4/k_0)\sin\theta_0 + 1}$$

$$\sim 2 - 2\sqrt{\omega\varepsilon_0/\left(i\sigma_4\right)}\csc\theta_0$$

$$A_0 \sim E\left(\omega\right)\sin\theta_0\left(1 - R_H\right) \sim E\left(0\right)\frac{2}{(k_4/k_0)\sin\theta_0 + 1}\sin\theta_0$$

$$\sim 2E(0)\sqrt{\omega\varepsilon_0/(i\sigma_4)}$$

$$A_4 \sim E(0)\frac{2}{(k_4/k_0)}\frac{(k_4/k_0)\sin\theta_0}{(k_4/k_0)\sin\theta_0+1}e^{-ihk_4}$$

$$\sim 2E(0)\sqrt{\omega\varepsilon_0/(i\sigma_4)}$$

$$I \sim -\frac{YA_0}{k_L^2-k_0^2\cos^2\theta_0} \sim -\frac{-i\omega C_e 2E(0)\sqrt{-i\omega\varepsilon_0/\sigma_4}}{\omega^2 C_e\frac{\mu_0}{2\pi}\ln\left(\frac{4h_{eff}}{e^{\gamma}ha\sqrt{-i\omega\mu_0\sigma_4}}\right)-\omega^2\mu_0\varepsilon_0\cos^2\theta_0}\ ,\ h\geq b$$

$$\sim \frac{1}{\sqrt{-i\omega}}\frac{-C_e 2E(0)\sqrt{\varepsilon_0/\sigma_4}}{-C_e\frac{\mu_0}{2\pi}\ln\left(\frac{4h_{eff}}{e^{\gamma}ha\sqrt{-i\omega\mu_0\sigma_4}}\right)+\mu_0\varepsilon_0\cos^2\theta_0}\ ,\ h\geq b$$

$$\sim \frac{1}{\sqrt{-i\omega}}\frac{-C_e 2E(0)\sqrt{\varepsilon_0/\sigma_4}}{-C_e\frac{\mu_0}{2\pi}\ln\left(\frac{4h_{eff}}{e^{\gamma}ba\sqrt{-i\omega\mu_0\sigma_4}}\right)+\mu_0\varepsilon_0\cos^2\theta_0}\ ,\ h<-b$$

$$\sim \frac{1}{\sqrt{-i\omega}}\frac{c_1}{-C_e\frac{\mu_0}{2\pi}\ln\left(c_2\sqrt{-i\omega}\right)} = \frac{1}{\sqrt{s}}\frac{c_1}{-C_e\frac{\mu_0}{2\pi}\ln\left(c_2\sqrt{s}\right)}$$

$$c_1 = C_e 2E(0)\sqrt{\varepsilon_0/\sigma_4}$$

$$c_2 = \frac{e^{\gamma}ha\sqrt{\mu_0\sigma_4}}{4h_{eff}}e^{2\pi(\varepsilon_0/C_e)\cos^2\theta_0}\ ,\ h\geq b$$

$$= \frac{e^{\gamma}ba\sqrt{\mu_0\sigma_4}}{4h_{eff}}e^{2\pi(\varepsilon_0/C_e)\cos^2\theta_0}\ ,\ h<-b$$

We have

$$I(-\omega) = I^*(\omega)$$

The current in the time domain is

$$I(t) = \frac{1}{2\pi}\int_{-\infty}^{\infty} e^{-i\omega t}I(\omega)\,d\omega$$

$$= \frac{1}{2\pi}\int_{-\infty}^{\infty}\cos(\omega t)\,I(\omega)\,d\omega - \frac{i}{2\pi}\int_{-\infty}^{\infty}\sin(\omega t)\,I(\omega)\,d\omega$$

Then

$$I(t) = \frac{1}{\pi}\int_0^\infty \cos(\omega t)\,\mathrm{Re}\{I(\omega)\}\,d\omega + \frac{1}{\pi}\int_0^\infty \sin(\omega t)\,\mathrm{Im}\{I(\omega)\}\,d\omega$$

$$\mathrm{Re}\{I(\omega)\} = \frac{1}{2}\left[I(\omega) + I(-\omega)\right] \sim \frac{1}{\sqrt{-i\omega}}\frac{c_1/2}{-C_e\frac{\mu_0}{2\pi}\ln\left(c_2\sqrt{-i\omega}\right)} + \frac{1}{\sqrt{i\omega}}\frac{c_1/2}{-C_e\frac{\mu_0}{2\pi}\ln\left(c_2\sqrt{i\omega}\right)}$$

$$\sim \frac{c_1}{\sqrt{2\omega}\left(-C_e\frac{\mu_0}{2\pi}\right)}\left[\frac{\ln\left(c_2\sqrt{\omega}\right) - \pi/4}{\left\{\ln^2\left(c_2\sqrt{\omega}\right) + \pi^2/4^2\right\}}\right]$$

$$\mathrm{Im}\{I(\omega)\} = \frac{1}{2}\left[I(\omega) - I(-\omega)\right] \sim \frac{1}{\sqrt{-i\omega}}\frac{c_1/2}{-C_e\frac{\mu_0}{2\pi}\ln\left(c_2\sqrt{-i\omega}\right)} - \frac{1}{\sqrt{i\omega}}\frac{c_1/2}{-C_e\frac{\mu_0}{2\pi}\ln\left(c_2\sqrt{i\omega}\right)}$$

$$\sim i\frac{c_1}{\sqrt{2\omega}\left(-C_e\frac{\mu_0}{2\pi}\right)}\left[\frac{\ln\left(c_2\sqrt{\omega}\right) + \pi/4}{\left\{\ln^2\left(c_2\sqrt{\omega}\right) + \pi^2/4^2\right\}}\right]$$

Thus the real part gives

$$\frac{1}{\pi}\int_0^R \cos(\omega t)\,\mathrm{Re}\{I(\omega)\}\,d\omega \sim \frac{1}{\pi}\frac{c_1}{\sqrt{2}\left(-C_e\frac{\mu_0}{2\pi}\right)}\int_0^R\left[\frac{\ln\left(c_2\sqrt{\omega}\right) - \pi/4}{\left\{\ln^2\left(c_2\sqrt{\omega}\right) + \pi^2/4^2\right\}}\right]\frac{d\omega}{\sqrt{\omega}}$$

$$\sim \frac{1}{\pi}\frac{\sqrt{2}c_1/c_2}{\left(-C_e\frac{\mu_0}{2\pi}\right)}\int_0^{c_2\sqrt{R}}\frac{\ln(u) - \pi/4}{\left\{\ln^2(u) + \pi^2/4^2\right\}}du$$

and the imaginary part gives

$$\frac{1}{\pi}\int_0^\infty \sin(\omega t)\,\mathrm{Im}\{I(\omega)\}\,d\omega \sim \frac{1}{\pi}\frac{c_1 t}{\sqrt{2}\left(-C_e\frac{\mu_0}{2\pi}\right)}\int_0^R\left[\frac{\ln\left(c_2\sqrt{\omega}\right) + \pi/4}{\left\{\ln^2\left(c_2\sqrt{\omega}\right) + \pi^2/4^2\right\}}\right]\sqrt{\omega}d\omega$$

$$\sim \frac{1}{\pi}\frac{t\sqrt{2}c_1/c_2^3}{\left(-C_e\frac{\mu_0}{2\pi}\right)}\int_0^{c_2\sqrt{R}}\frac{\ln(u) + \pi/4}{\left\{\ln^2(u) + \pi^2/4^2\right\}}u^2du$$

9 BELL LABS EMP WAVEFORM

The Bell Labs electromagnetic pulse waveform will be taken as excitation of the transmission line. A double exponential characterization of the waveform is [11]

$$E(t) = E_0\left(e^{-\alpha t} - e^{-\beta t}\right)u(t)$$

where

$$E_0 = 52.5 \text{ kV/m}$$

$$\alpha = 4\times 10^6 \text{ s}^{-1}$$

$$\beta = 4.76 \times 10^8 \text{ s}^{-1}$$

The peak amplitude is 50 kV/m, with a 10% to 90% rise time of 4.15 ns, and a fall time from peak to 50% of peak of 175 ns. The spectrum is

$$E(\omega) = \int_{-\infty}^{\infty} E(t) e^{i\omega t} dt = \frac{E_0 (\beta - \alpha)}{(\alpha - i\omega)(\beta - i\omega)}$$

The double exponential waveform has a discontinuity in slope at $\omega = 0$ which artificially enhances the high frequencies. It is sometimes more convenient to use a fit without this discontinuity

$$E(t) = E_0 \frac{de^{\alpha t}}{1 + e^{\beta(t - t_p)}}$$

The choice of parameters which fit the peak amplitude and the rise and fall times of the Bell Labs waveform are [21]

$$\alpha = 10.3 \times 10^8 s^{-1}$$

$$\beta = 10.34 \times 10^8 \text{ s}^{-1}$$

$$d = 1.160227115 \times 10^{-9}$$

$$t_p = 20 \text{ ns}$$

$$E_0 = 50 \text{ kV/m}$$

The corresponding spectrum is

$$E(\omega) = E_0 d \frac{\pi}{\beta} \frac{e^{(\alpha + i\omega) t_p}}{\sin[(\alpha + i\omega)\pi/\beta]}$$

10 SIMULATION RESULTS

The parameters we take on the simulations [8]

$$\varepsilon_{r4} = \varepsilon_4 / \varepsilon_0 = 20$$

$$\sigma_4 = 0.01 \text{ S/m}$$

$$\varepsilon_0 = 8.854 \times 10^{-12} \text{ F/m}$$

$$\mu_0 = 4\pi \times 10^{-7} \text{ H/m}$$

and as an example

$$\varepsilon_{r2} = \varepsilon_2/\varepsilon_0 = 3$$

$$a = 1 \text{ cm}$$

$$b = 2 \text{ cm}$$

For the wire above the ground we use [7]

$$h = 10 \text{ m}$$

on the ground we use

$$h = b$$

and below the ground we use as an example

$$h = -3 \text{ m}$$

The results for the time domain current are shown in Figure 13. The angles of incidence are near the value which produces the maximum current peak. When the wire is high above the ground the peak current level is achieved near grazing incidence ($\theta_0 \to 0$). When the wire is resting on the ground, normal incidence ($\theta_0 \to \pi/2$) gives near the peak level (green curve). When the wire is buried, normal incidence yields the peak level ($\theta_0 = \pi/2$). If the insulation is removed ($\varepsilon_{r2} \to 1$) then the current peak is larger in the overhead case (blue curve) because of the slightly small value of k_L and resulting near cancellation of the denominator of the current formula near grazing.

10.1 Comparison of Exact Filament Current and Transmission Line Current

The inverse transform of the exact filament current was also carried out for the filament (without insulation) above the ground. Figure 14 shows the case with $\sigma_4 = 0.01$ S/m. These two curves close to the results reported by Tesche [18].

Figure 15 shows the case with $\sigma_4 = 0.1$ S/m.

Finally Figure 16 shows the case with $\sigma_4 = 0.001$ S/m

There is some error for the small conductivity cases, but the transmission line clearly yields a useful approximation.

11 APPROXIMATE TRANSFORM

We use the decaying exponential in this section with transform

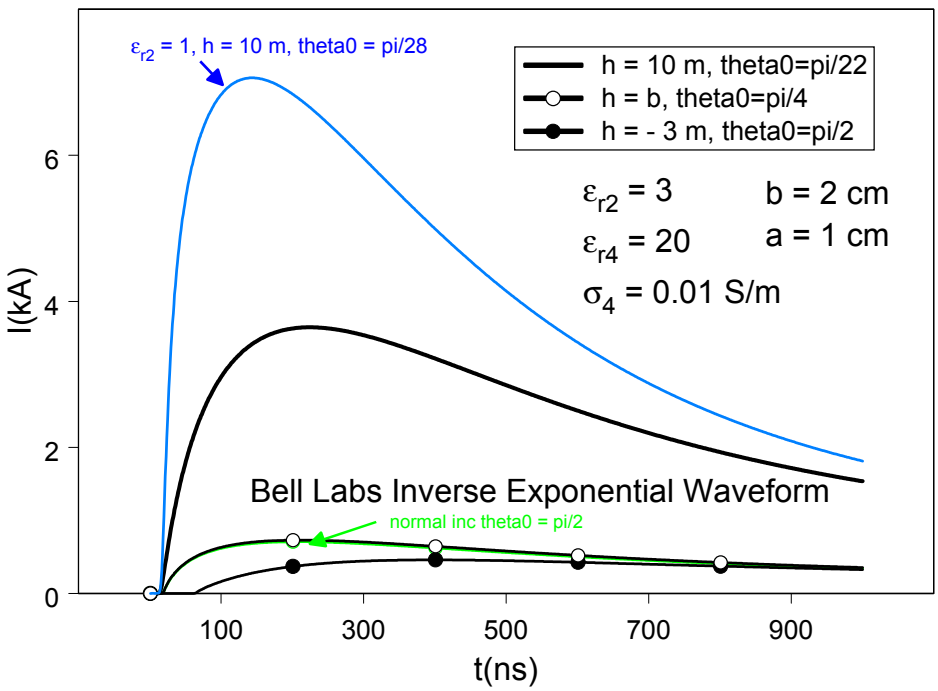

Figure 13. Transmission line model for time domain current. The blue curve is the case where the wire does not have insulation and is above ground (the incident angle was adjusted for maximum peak level, which occurs near the grazing angle). The black curve is the insulated wire (again the incident angle gives peak current). The black curve with open circles is the case where the wire is resting on the ground (again the indicent angle gives peak current, however the current in this case is insensitive to incident angle as shown by the normally incident green result). The black curve with closed circles is the buried case (normal incidence results in the maximimum current, but again the curve is insensitive to incident angle).

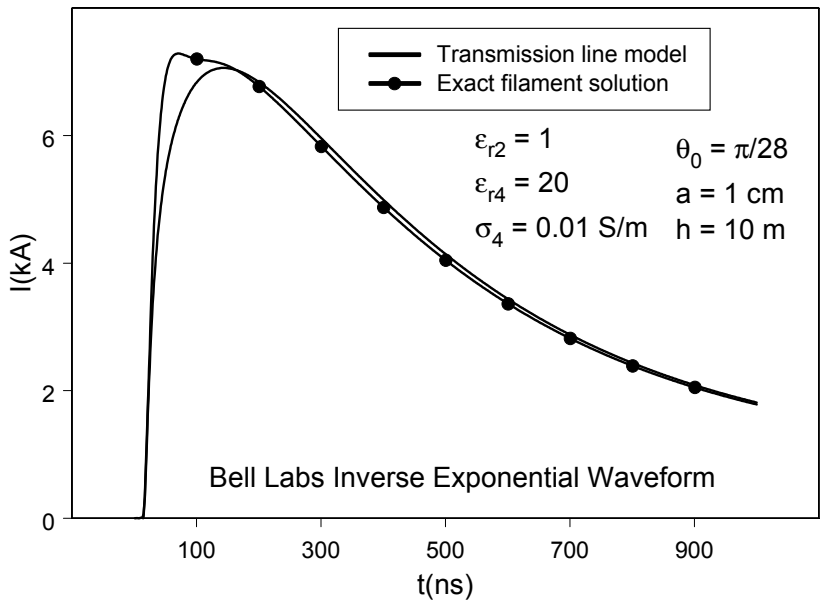

Figure 14. Comparison of exact filament result and transmission line result for the wire without insulation above ground near the grazing incidence angle. The ground conductivity in this case was $\sigma_4 = 0.01$ S/m.

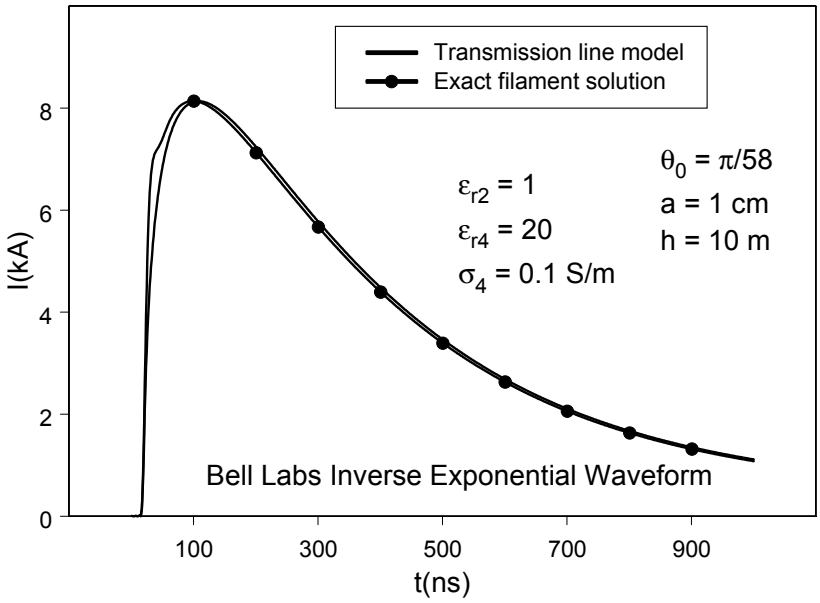

Figure 15. Comparison of exact filament result and transmission line result for the wire without insulation above ground near the grazing incidence angle. The ground conductivity in this case was $\sigma_4 = 0.1$ S/m.

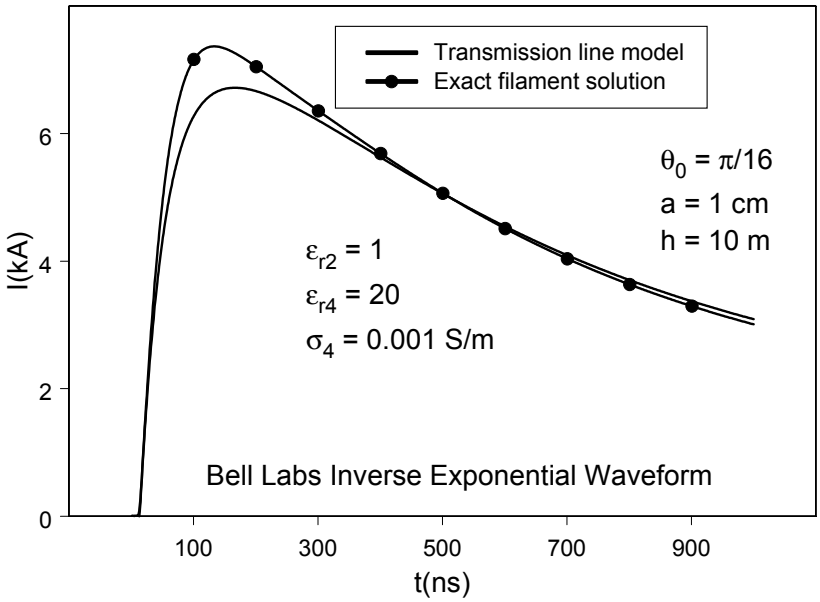

Figure 16. Comparison of exact filament result and transmission line result for the wire without insulation above ground near the grazing incidence angle. The ground conductivity in this case was $\sigma_4 = 0.001$ S/m.

$$E(\omega) = E_0/(\alpha - i\omega)$$

where $E_0 = 50$ kV/m and $\alpha = 4 \times 10^6$ s^{-1}. The case where the insulation radius h or b is electrically thin $k_0 h, k_2 b << 1$ (where $k_2 = \omega\sqrt{\mu_0 \varepsilon_2}$) can be inverse transformed approximately.

$$Z = Z_e + Z_4$$

$$Z_e = -i\omega L_e = sL_e$$

$$L_e = L_2 + L_0$$

$$L_2 = \frac{\mu_0}{2\pi} \ln(b/a)$$

$$L_0 = \frac{\mu_0}{2\pi} \text{Arccosh}(h/b)$$

$$Z_4 \approx -i\omega \frac{\mu_0}{2\pi} \ln\left(\frac{1 - ik_4 h}{-ik_4 h}\right) = s\frac{\mu_0}{2\pi} \ln\left(\frac{1 - ik_4 h}{-ik_4 h}\right), \; h \geq b$$

$$\approx -i\omega \frac{\mu_0}{2\pi} \ln\left(\frac{1 - ik_4 b}{-ik_4 b}\right) = s\frac{\mu_0}{2\pi} \ln\left(\frac{1 - ik_4 b}{-ik_4 b}\right), \; h < b$$

(note here that the numerical curves remain the essentially the same regardless of whether Sunde's logarithmic approximation, Vance's Hankel function approximation, or Carson's integral formula are used for the ground impedance)

$$k_4 = \sqrt{\omega\mu_0(\omega\varepsilon_4 + i\sigma_4)} = \sqrt{-s\mu_0(\sigma_4 + s\varepsilon_4)}$$

$$k_0 = \sqrt{\omega^2 \mu_0 \varepsilon_0} = \sqrt{-s\mu_0 s\varepsilon_0}$$

$$s = -i\omega$$

$$I = -\frac{YA_n e^{izk_0 \cos\theta_0}}{k_L^2 - k_0^2 \cos^2\theta_0}$$

$$Y = \frac{Y_e Y_4}{Y_e + Y_4}$$

$$Y_e = -i\omega C_e = sC_e$$

$$Y_4 \approx (\sigma_4 - i\omega\varepsilon_4)\pi/\ln\left(\frac{1 - ik_4 h}{-ik_4 h}\right) = (\sigma_4 + s\varepsilon_4)\pi/\ln\left(\frac{1 - ik_4 h}{-ik_4 h}\right), \; h \geq b$$

$$\approx (\sigma_4 - i\omega\varepsilon_4)\, 2\pi / \left[\ln\left(\frac{1 - ik_4 b}{-ik_4 b}\right) + \ln\left(\frac{1 - ik_4\sqrt{b^2+4h^2}}{-ik_4\sqrt{b^2+4h^2}}\right)\right]$$

$$= (\sigma_4 + s\varepsilon_4)\, 2\pi / \left[\ln\left(\frac{1 - ik_4 b}{-ik_4 b}\right) + \ln\left(\frac{1 - ik_4\sqrt{b^2+4h^2}}{-ik_4\sqrt{b^2+4h^2}}\right)\right] \text{ , } h < -b$$

(note here that the numerical curves remain essentially the same if the ground admittance is ignored when the insulation around the wire is sufficiently thick)

$$k_L^2 = -ZY$$

$$A_0 = E(s)\sin\theta_0 \left[e^{-ihk_0\sin\theta_0} - R_H e^{ihk_0\sin\theta_0}\right]$$

$$R_H = \frac{(k_4/k_0)^2 \sin\theta_0 - \sqrt{(k_4/k_0)^2 - \cos^2\theta_0}}{(k_4/k_0)^2 \sin\theta_0 + \sqrt{(k_4/k_0)^2 - \cos^2\theta_0}}$$

$$I(s) = \frac{YA_n e^{izk_0\cos\theta_0}}{ZY + k_0^2\cos^2\theta_0}$$

$$= \frac{A_n e^{izk_0\cos\theta_0}}{Z + (k_0^2/Y)\cos^2\theta_0}$$

If we assume that $k_0 h << 1$

$$A_0 \sim E(s)\sin\theta_0 \left[1 - R_H\right]$$

$$1 - R_H = \frac{2\sqrt{(k_4/k_0)^2 - \cos^2\theta_0}}{(k_4/k_0)^2 \sin\theta_0 + \sqrt{(k_4/k_0)^2 - \cos^2\theta_0}}$$

If we assume $k_4/k_0 >> 1$

$$R_H \sim \frac{(k_4/k_0)\sin\theta_0 - 1}{(k_4/k_0)\sin\theta_0 + 1}$$

$$1 - R_H \sim \frac{2}{(k_4/k_0)\sin\theta_0 + 1}$$

The inverse transform has the form

$$I(t) = \frac{1}{2\pi i}\int_{c-i\infty}^{c+i\infty} I(s)\, e^{st} ds$$

Now at $z = 0$

$$I(t) \sim \frac{1}{2\pi i}\int_{c-i\infty}^{c+i\infty} \frac{\sin\theta_0\left[1-R_H\right]}{Z+\left(k_0^2/Y\right)\cos^2\theta_0} E(s)\, e^{st} ds$$

$$\sim \frac{1}{2\pi i}\int_{c-i\infty}^{c+i\infty} \frac{\sin\theta_0}{Z+\left(k_0^2/Y\right)\cos^2\theta_0} \frac{2}{\left(k_4/k_0\right)\sin\theta_0+1} E(s)\, e^{st} ds$$

$$Z = Z_e + Z_4$$

$$1/Y = 1/Y_e + 1/Y_4$$

$$I(t) \sim \frac{1}{2\pi i}\int_{c-i\infty}^{c+i\infty} \frac{\sin\theta_0}{Z_e+\left(k_0^2/Y_e\right)\cos^2\theta_0 + Z_4 + \left(k_0^2/Y_4\right)\cos^2\theta_0}$$

$$\frac{2}{\left(k_4/k_0\right)\sin\theta_0+1} E(s)\, e^{st} ds$$

$$\sim \frac{1}{2\pi i}\int_{c-i\infty}^{c+i\infty} \frac{\sin\theta_0}{Z_e/s+\left\{\left(k_0^2/s^2\right)/\left(Y_e/s\right)\right\}\cos^2\theta_0 + Z_4/s + \left\{\left(k_0^2/s^2\right)/\left(Y_4/s\right)\right\}\cos^2\theta_0}$$

$$\frac{2}{\left(k_4/k_0\right)\sin\theta_0+1} E(s)\, e^{st} \frac{ds}{s}$$

Let us write this as

$$I(t) \sim \frac{1}{2\pi i}\int_{c-i\infty}^{c+i\infty} \frac{\sin\theta_0}{Z_e/s+\left\{\left(k_0^2/s^2\right)/\left(Y_e/s\right)\right\}\cos^2\theta_0 + Z_4/s + \left\{\left(k_0^2/s^2\right)/\left(Y_4/s\right)\right\}\cos^2\theta_0}$$

$$\frac{2/\sqrt{s}}{\left(k_4/k_0\right)\sin\theta_0+1} E(s)\, e^{st} \frac{ds}{\sqrt{s}}$$

The source factor is taken as the transform

$$E_i(t) = \frac{1}{2\pi i}\int_{c-i\infty}^{c+i\infty} E(s)\, e^{st} \frac{ds}{\sqrt{s}} = E_0 \frac{1}{2\pi i}\int_{c-i\infty}^{c+i\infty} e^{st} \frac{ds}{(s+\alpha)\sqrt{s}}$$

$$= E_0 \frac{2}{\sqrt{\pi\alpha}} F\left(\sqrt{\alpha t}\right) = E_0 f(t)$$

where F is Dawson's integral [22]

$$F(z) = e^{-z^2}\int_0^z e^{\lambda^2} d\lambda = \frac{1}{2} e^{-z^2}\int_0^{z^2} e^u \frac{du}{\sqrt{u}} = \frac{1}{2}\int_0^{z^2} e^{-u} \frac{du}{\sqrt{z^2-u}}$$

The small and large argument forms of this function are

$$F(z) = z\left[1 + \frac{\left(-2z^2\right)}{1\cdot 3} + \frac{\left(-2z^2\right)^2}{1\cdot 3\cdot 5} + \cdots\right]$$

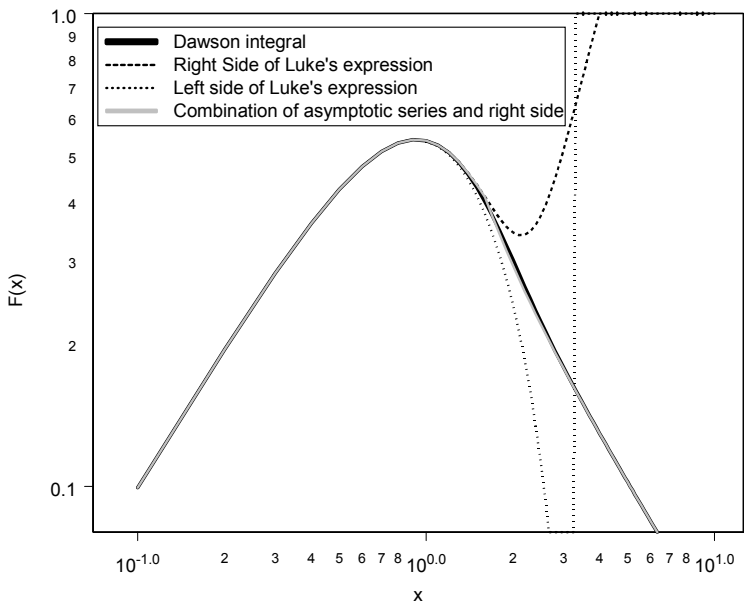

Figure 17. Comparisons of Dawson integral function with simple fit functions and combination of simple fit function and asymptotic approximation.

$$F(z) \sim \frac{1}{2z}\left[1+\frac{1}{2z^2}+\frac{1\cdot 3}{(2z^2)^2}+\cdots\right],\ z\to\infty$$

Also we can write [23]

$$\frac{105-10z^2}{105+60z^2+12z^4} < F(z)/z < \frac{945-210z^2+32z^4}{945+420z^2+60z^4}$$

We can use, say, the asymptotic form (with three terms) for $z > 1.6009476$ (the intersection point) and the right side of the preceding expression for $z \leq 1.6009476$ as shown as the grey curve in Figure 17.

The impedance factor is taken as

$$Y_e/s = C_e$$

$$Z_e/s = L_e$$

$$k_0^2/s^2 = -\mu_0\varepsilon_0$$

$$-ik_4 = \sqrt{-i\omega\mu_0\left(-i\omega\varepsilon_4+\sigma_4\right)} = \sqrt{s\mu_0\left(\sigma_4+s\varepsilon_4\right)}$$

$$k_4/k_0 = \sqrt{\frac{\sigma_4/s + \varepsilon_4}{\varepsilon_0}}$$

$$Z_4/s \approx \frac{\mu_0}{2\pi} \ln \left[\frac{1 + h\sqrt{s\mu_0 (\sigma_4 + s\varepsilon_4)}}{h\sqrt{s\mu_0 (\sigma_4 + s\varepsilon_4)}} \right]$$

$$Y_4/s \approx (\sigma_4/s + \varepsilon_4)\, \pi / \ln \left[\frac{1 + h\sqrt{s\mu_0 (\sigma_4 + s\varepsilon_4)}}{h\sqrt{s\mu_0 (\sigma_4 + s\varepsilon_4)}} \right]$$

The key step in the approximation is to replace $1/s$ in the impedance and reflection factors by an average [24]

$$\langle 1/s \rangle = \frac{1}{2\pi i} \int_{c-i\infty}^{c+i\infty} s^{-3/2} (s+\alpha)^{-1} e^{st} ds / \frac{1}{2\pi i} \int_{c-i\infty}^{c+i\infty} s^{-1/2} (s+\alpha)^{-1} e^{st} ds$$

$$= \int_0^t f(\tau)\, d\tau / f(t)$$

where we can write this ratio as

$$\frac{1}{f(t)} \int_0^t f(\tau)\, d\tau = \frac{1}{\alpha} \left[\frac{2}{f(t)\sqrt{\pi/t}} - 1 \right] = \frac{1}{\alpha} \left[\frac{\sqrt{\alpha t}}{F\left(\sqrt{\alpha t}\right)} - 1 \right]$$

The expansions are

$$\frac{1}{f(t)} \int_0^t f(\tau)\, d\tau \sim \frac{2}{3} t \left(1 + \frac{4}{15} \alpha t + \cdots \right) \ , \ \alpha t \to 0$$

$$\frac{1}{f(t)} \int_0^t f(\tau)\, d\tau \sim 2t \left[1 - 1/(\alpha t) + \cdots \right] \ , \ \alpha t \to \infty$$

However in the overhead case we simplify further by taking (actually the presence of a finite Y_4 only has an impact in the cases where the wire is resting on the ground or below ground when the insulation of the wire is much thinner than taken in this report)

$$Y_4 \to \infty$$

and thus

$$Z_4/s \approx \frac{\mu_0}{2\pi} \ln \left[1 + \frac{\langle 1/s \rangle}{h\sqrt{\mu_0 (\sigma_4 \langle 1/s \rangle + \varepsilon_4)}} \right]$$

$$(1 - R_H)/\sqrt{s} \approx \frac{2\sqrt{\langle 1/s \rangle}}{\sqrt{(\sigma_4 \langle 1/s \rangle + \varepsilon_4)/\varepsilon_0} \sin\theta_0 + 1}$$

$$I(t) \approx \frac{\sin\theta_0}{L_e - (\mu_0 \varepsilon_0 / C_e) \cos^2\theta_0 + Z_4/s} (1 - R_H)/\sqrt{s}$$

$$E_0 \frac{2}{\sqrt{\pi\alpha}} F\left(\sqrt{\alpha t}\right)$$

This approximation yields the dashed curves in the Figures. The incident angles shown give maximum current peaks.

11.1 Below Ground Case

The below ground case is addressed by inserting the factor

$$e^{-ih\sqrt{k_4^2-k_0^2\cos^2\theta_0}} \sim e^{-ihk_4} = \exp\left[h\sqrt{s\mu_0\left(\sigma_4+s\varepsilon_4\right)}\right]$$

into the integrand (here $h<0$). We can limit consideration to normal incidence since this is typically the maximum

$$I(t) \approx \frac{1}{2\pi i}\int_{c-i\infty}^{c+i\infty} \frac{1}{L_2+Z_4/s} \frac{2e^{h\left\{\sqrt{s\mu_0(\sigma_4+s\varepsilon_4)}-\sqrt{s\mu_0\sigma_4}\right\}}}{\sqrt{\left(\sigma_4+s\varepsilon_4\right)/\varepsilon_0}+\sqrt{s}} e^{h\sqrt{s\mu_0\sigma_4}} E(s)\, e^{st}\frac{ds}{\sqrt{s}}$$

$$\approx E_0 \frac{1}{2\pi i}\int_{c-i\infty}^{c+i\infty} \frac{1}{L_2+Z_4/s} \frac{2e^{h\left\{\sqrt{s\mu_0(\sigma_4+s\varepsilon_4)}-\sqrt{s\mu_0\sigma_4}\right\}}}{\sqrt{\left(\sigma_4+s\varepsilon_4\right)/\varepsilon_0}+\sqrt{s}} e^{st-\sqrt{s\tau}}\frac{ds}{(s+\alpha)\sqrt{s}}$$

where

$$\tau = h^2\mu_0\sigma_4$$

We now use a simple average value $\langle 1/s\rangle \to 2t$ in the impedance and reflection coefficient factors (this is the late time limit of the average in the previous section). Of course it would be more consistent to use the average defined in the previous section with the addition of the added exponential term. The ground admittance Y_4 can also be added if very thin wire insulations are considered. Then

$$I(t) \approx \frac{1}{L_2+Z_4/s} \frac{2e^{h\left\{\sqrt{s\mu_0(\sigma_4+s\varepsilon_4)}-\sqrt{s\mu_0\sigma_4}\right\}}}{\sqrt{\left(\sigma_4+s\varepsilon_4\right)/\varepsilon_0}+\sqrt{s}} E_0 \frac{1}{2\pi i}\int_{c-i\infty}^{c+i\infty} e^{st-\sqrt{s\tau}}\frac{ds}{(s+\alpha)\sqrt{s}}$$

We factor

$$\frac{1}{s+\alpha} = \frac{1}{i2\sqrt{\alpha}}\left(\frac{1}{\sqrt{s}-i\sqrt{\alpha}} - \frac{1}{\sqrt{s}+i\sqrt{\alpha}}\right)$$

Using an identity from [22] gives

$$I(t) \approx \frac{1}{L_2+Z_4/s} \frac{2\sqrt{\langle 1/s\rangle}e^{h\left\{\sqrt{\mu_0(\sigma_4\langle 1/s\rangle+\varepsilon_4)}-\sqrt{\mu_0\sigma_4\langle 1/s\rangle}\right\}/\langle 1/s\rangle}}{\sqrt{\left(\sigma_4\langle 1/s\rangle+\varepsilon_4\right)/\varepsilon_0}+1} E_0$$

$$\frac{e^{-\alpha t}}{\sqrt{\alpha}}\,\mathrm{Im}\left[e^{-i\sqrt{\alpha\tau}}\mathrm{erfc}\left(\frac{1}{2}\sqrt{\tau/t}-i\sqrt{\alpha t}\right)\right]$$

where

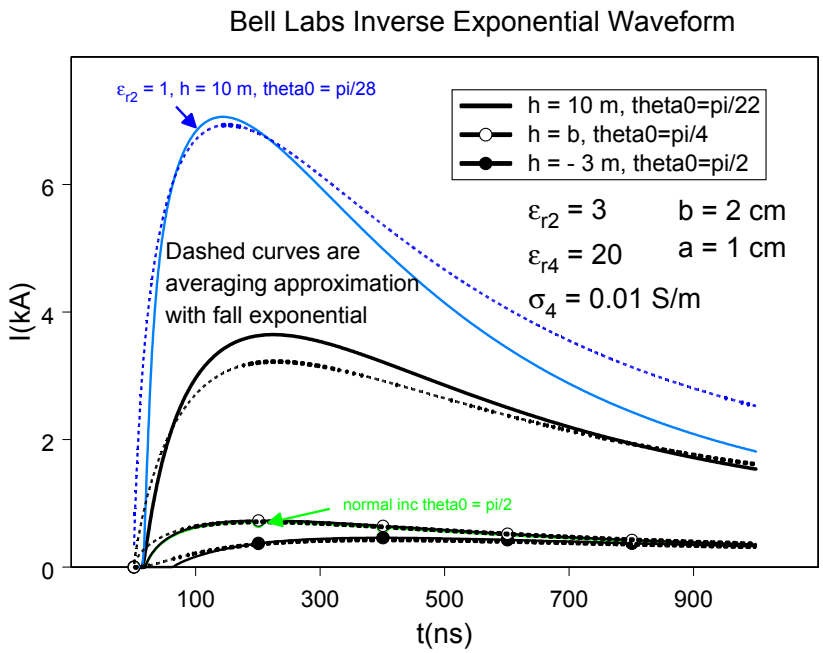

Figure 18. Comparison of transmission line results with averaging approximation to inverse Laplace transform of transmission line results (dashed curves) for $\sigma_4 = 0.01$ S/m.

$$Z_4/s \approx \frac{\mu_0}{2\pi} \ln \left[1 + \frac{\langle 1/s \rangle}{h\sqrt{\mu_0 \left(\sigma_4 \langle 1/s \rangle + \varepsilon_4 \right)}} \right]$$

Note that various approximations are available for the error function with complex arguments [25].

11.2 Results

The main error at early time in Figures 18, 19, and 20 is caused by the fact that the causal delay time for the incident wave (both the start of the inverse exponential and the underground propagation) was not included in the approximation (this could have been directly taken into account by extracting an exponential factor in the transform for high frequencies and including it in the kernel as a time shift). This shift can be taken into account on all approximate curves by simply delaying the start of the approximate waveform by the appropriate amount (say, twenty nanoseconds for the inverse exponential and the appropriate high frequency propagation delay time)

$$\Delta t \approx 20 \text{ ns} - h \sin\theta_0 / c \,,\; h > 0$$

$$\approx 20 \text{ ns} - h\sqrt{\varepsilon_{r4}}/c \,,\; h < 0 \,,\; \theta_0 = \pi/2$$

where $c \approx 3 \times 10^8$ m/s is the vacuum velocity of light. This modification would improve the early time accuracy of all approximate curves as shown in figure 21, 22, and 23.

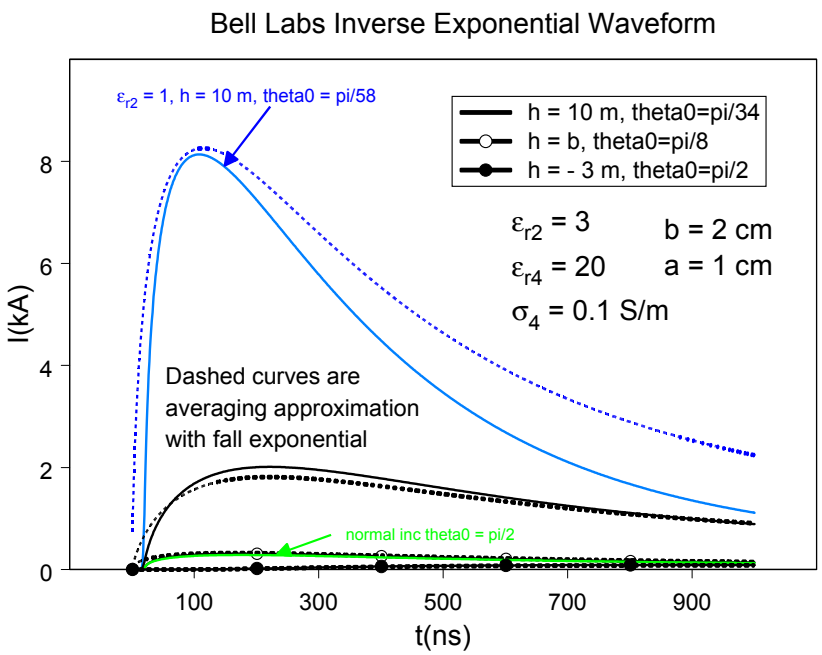

Figure 19. Comparison of transmission line results with averaging approximation to inverse Laplace transform of transmission line results (dashed curves) for $\sigma_4 = 0.1$ S/m.

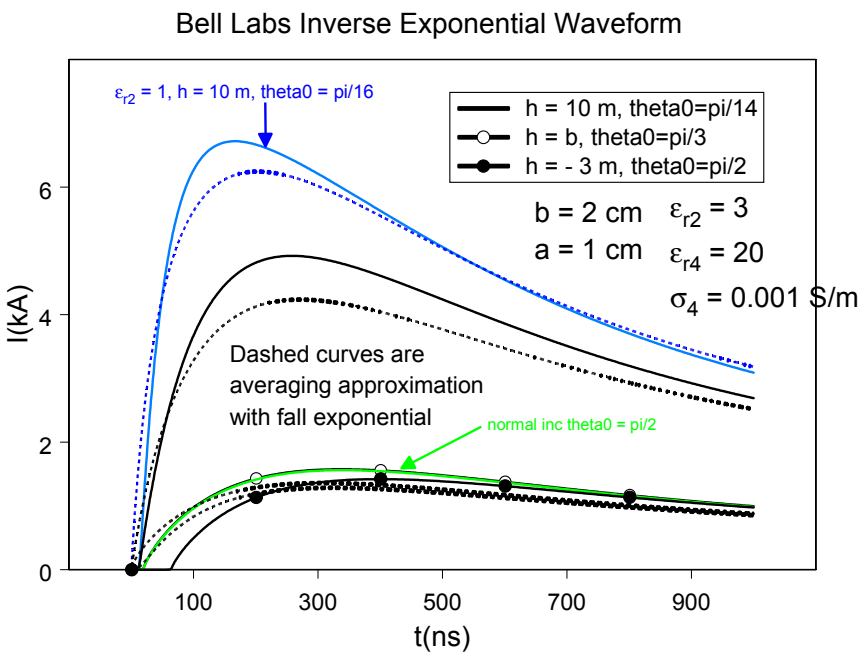

Figure 20. Comparison of transmission line results with averaging approximation to inverse Laplace transform of transmission line results (dashed curves) for $\sigma_4 = 0.001$ S/m.

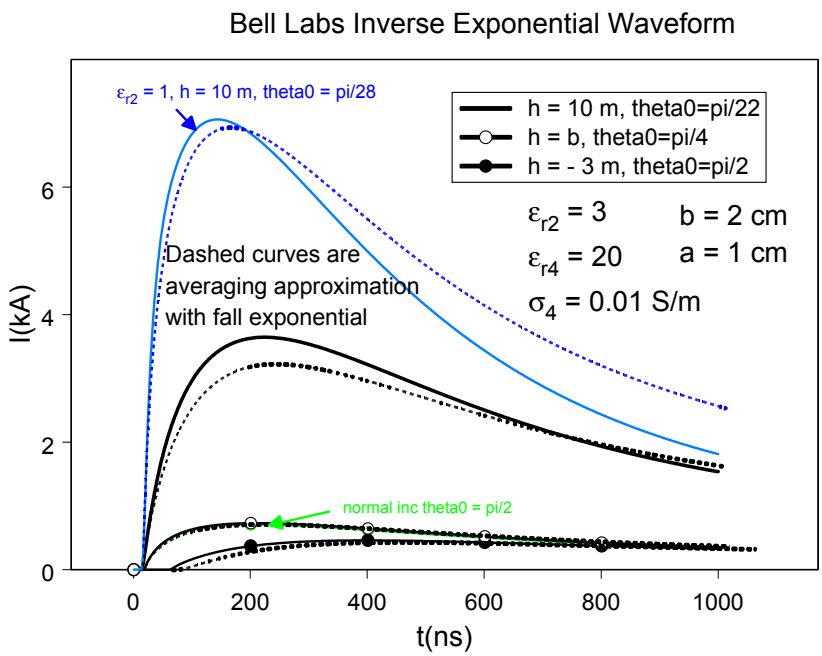

Figure 21. Comparison of transmission line results with averaging approximation to inverse Laplace transform of transmission line results (dashed curves) which have been shifted in time for $\sigma_4 = 0.01$ S/m.

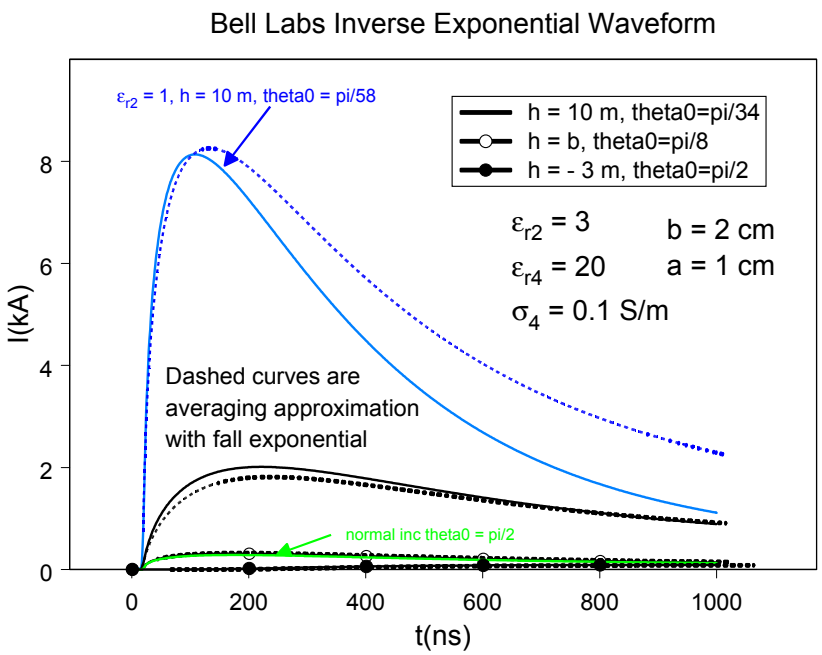

Figure 22. Comparison of transmission line results with averaging approximation to inverse Laplace transform of transmission line results (dashed curves) which have been shifted in time for $\sigma_4 = 0.1$ S/m.

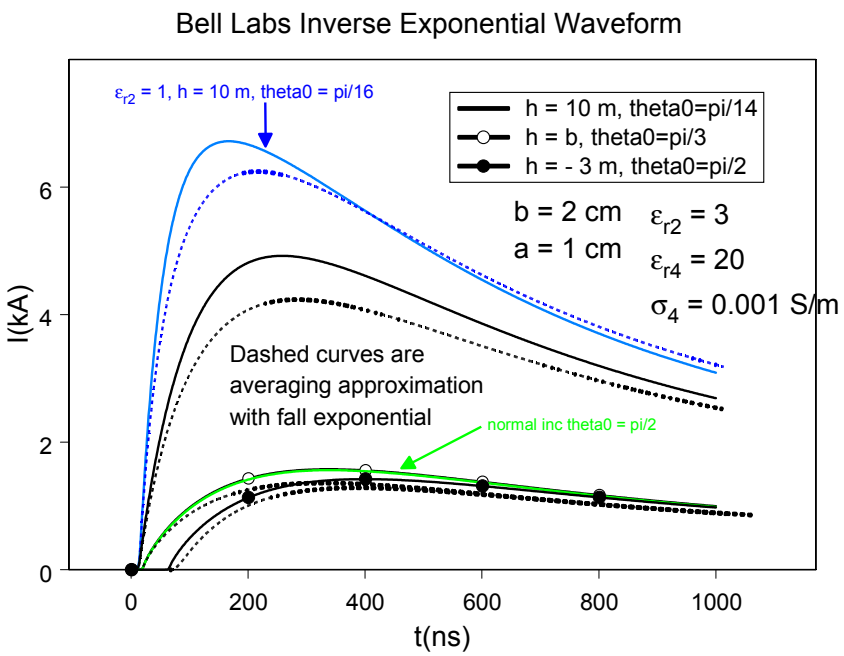

Figure 23. Comparison of transmission line results with averaging approximation to inverse Laplace transform of transmission line results (dashed curves) which have been shifted in time for $\sigma_4 = 0.001$ S/m.

12 SEMI-INFINITE LINE

The case where the line is semi-infinite is of interest in driving facilities. There is in general a drive from the incident field along the downward leg of the line (for example at grazing incidence) which typically reduces the current somewhat [12]. This contribution will not be included here because it is influenced by the termination details (angle of termination, whether a conduit is present). In this section we simply add the homogeneous solution of the transmission line current propagating in the backward direction

$$I = c_2 e^{-ik_L z} - \frac{Y A_n e^{izk_0 \cos\theta_0}}{k_L^2 - k_0^2 \cos^2\theta_0}$$

In the short circuit case, from the transmission line equation the derivative of the current at $z = 0$ must vanish. Thus c_2 is determined and the value of the short circuit current at the end is

$$I_{sc} = -\frac{Y A_n}{k_L^2 - k_0^2 \cos^2\theta_0}\left(1 + \frac{k_0 \cos\theta_0}{k_L}\right) = \frac{-A_n Y/k_L}{k_L - k_0 \cos\theta_0}$$

Because, in the overhead case we expect, near the grazing incidence peak, to have k_L be near $k_0 \cos\theta_0$, we anticipate a near doubling of the short circuit current over the infinite line current. Figure 24 shows the transmission line results for the infinite line current, the semi-infinite short circuit current, and one half the short circuit current (which aligns with the infinite line current in the overhead cases) for $\sigma_4 = 0.01$ S/m. Thus the doubling of the current occurs in the overhead cases but not when resting on the ground (which has a peak off normal incidence as noted in the figure, but is only slightly above the infinite line current. The below ground short circuit current was not plotted but is expected to be the same as the infinite line current.

When the semi-infinite line is open circuited we find the homogeneous solution coefficient c_2 to make the current vanish at $z = 0$. The open circuit voltage is then found to be

$$V_{oc} = \frac{iA_n}{k_L - k_0 \cos\theta_0} = Z_c I_{sc}$$

The source impedance is the characteristic impedance. When $h > 0$

$$Z_c = \sqrt{Z/Y} \approx \sqrt{\frac{L_e + Z_4/s}{C_e}}$$

where we have taken $Y_4 \to \infty$ and

$$Z_4/s \approx \frac{\mu_0}{2\pi} \ln\left[1 + \frac{\langle 1/s \rangle}{h\sqrt{\mu_0\left(\sigma_4 \langle 1/s \rangle + \varepsilon_4\right)}}\right]$$

When $h < 0$

$$Z_c = \sqrt{\frac{L_2 + Z_4/s}{C_2}}$$

where

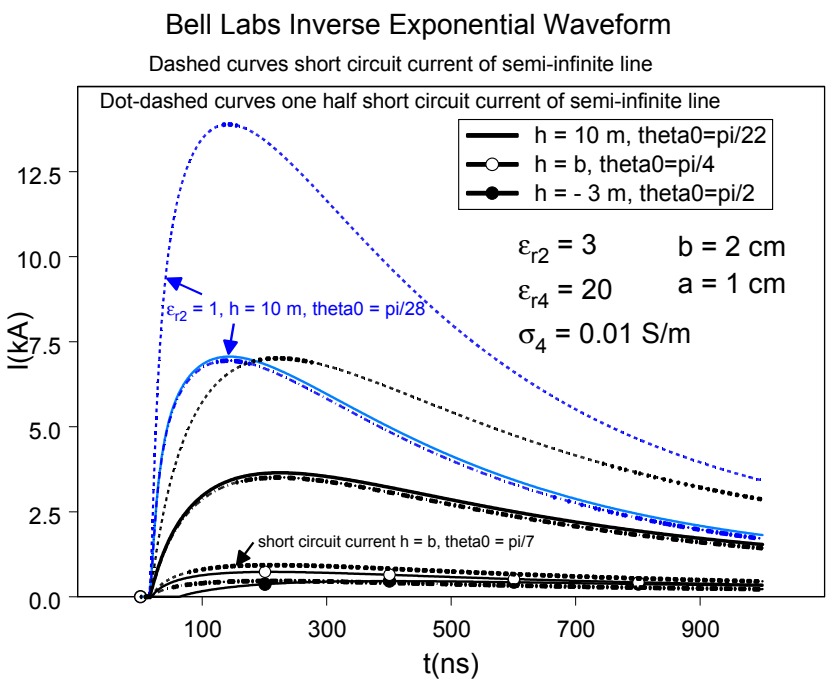

Figure 24. Comparison of transmission line results for infinite line currents (solid curves), semi-infinite short circuit currents (dashed curves), and one half the short circuit current (dot-dashed curves). The semi-infinite currents for the buried case were not plotted.

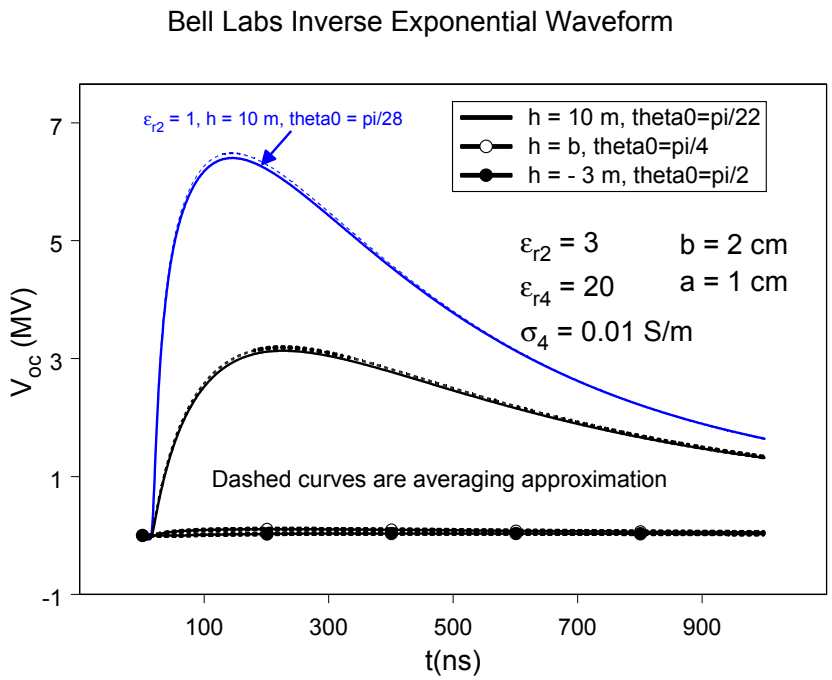

Figure 25. Open circuit voltage transmission line model results. Solid curves from inverse transform. Dashed curves are short circuit current multiplied by the time averaged approximation for impedance.

$$Z_4/s \approx \frac{\mu_0}{2\pi} \ln\left[1 + \frac{\langle 1/s \rangle}{b\sqrt{\mu_0\left(\sigma_4 \langle 1/s \rangle + \varepsilon_4\right)}}\right]$$

We can use the late time approximation

$$\langle 1/s \rangle \to 2t$$

in these expressions. Figure 25 shows the open circuit voltage using the transmission line model (solid curves). The dashed curves are the short circuit current times the approximate impedance using this average value of $1/s$. If the Dawson integral average is used the approximate above ground results are even closer to the solid curves. The causal time shift Δt can also be applied to the impedance (and makes physical sense) but it makes little difference in these voltage results because of the smoothness of the impedance function.

Figure 26 shows a comparison of the ratio of V_{oc} to I_{sc} to the time averaged characteristic impedance (again $2t$ is used for the average of the inverse of s). In this plot the causal time shift Δt was added to the impedance.

13 CONCLUSIONS

The current on a long insulated wire excited by an electromagnetic pulse is determined when the wire is above the ground, resting on the ground, and buried. The Bell Laboratories electromagnetic pulse waveform is used for excitation.

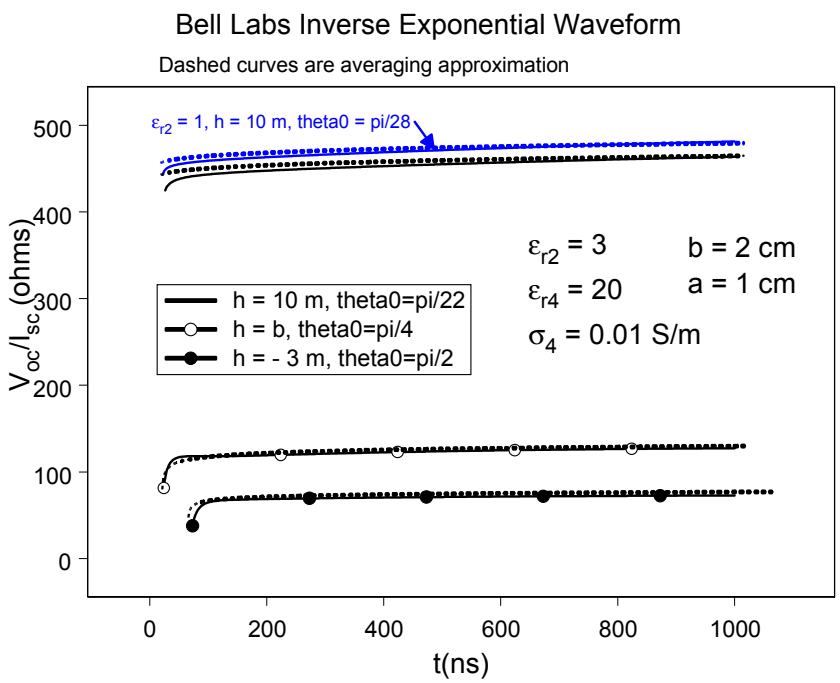

Figure 26. Ratio of open circuit voltage to short circuit current (solid curves) compared to time averaged characteristic impedance, which has been shifted in time by causal time shift (dashed curves).

The transmission line approximation is used to find the current. Wait's filament over ground solution is also used to benchmark the accuracy of the transmission line model. Approximate impedance per unit length and admittance per unit length formulas are considered and implemented. Finally, the inverse transform for the current is approximated by an averaging method to yield closed form results for the current on the wire.

It is shown that the semi-infinite line, short circuit current, approximately doubles over the infinite line current in the overhead cases (we have not included excitations of the vertical conductors in this calculation).

References

[1] J. R. Carson, "Wave Propagation in Overhead Wires with Ground Return," Bell System Technical Journal, Vol. 5, pp. 539-554, 1926.

[2] E. D. Sunde, **Earth Conduction Effects in Transmission Systems**, New York: Dover, 1967, p. 168.

[3] J. R. Wait, "Theory of wave propagation along a thin wire parallel to an interface," Radio Science, Vol. 7, No. 6, pp. 675-679, June 1972.

[4] J. R. Wait, "Tutorial Note on the General Transmission Line Theory for a Thin Wire Above the Ground," IEEE Transactions on Electromagnetic Compatibility, Vol. 33, No. 1, 1991.

[5] E. F. Kuester, D. C. Chang, S. W. Plate, "Electromagnetic Wave Propagation Along Horizontal Wire Systems In Or Near a Layered Earth," Electromagnetics, 1: 243-265, 1981.

[6] K. C. Chen, "Time Harmonic Solutions for a Long Horizontal Wire Over the Ground with Grazing Incidence," IEEE Transactions on Antennas and Propagation, Vol. AP-33, No. 3, March 1983.

[7] K. C. Chen, "EMP-Induced, Time-Domain Grazing Solution for an Infinite Wire Over the Ground," SAND85-0222, May 1985.

[8] K. C. Chen and L. K. Warne, "A Uniformly Valid Loaded Antenna Theory," IEEE Transactions on Antennas and Propagation, Vol. 40, No. 11, Nov. 1992.

[9] K. C. Chen and K. M. Damrau, "Accuracy of Approximate transmission Line Formulas for Overhead Wires," IEEE Transactions on Electromagnetic Compatibility, Vol. 31, No. 4, Nov. 1989.

[10] Yu. P. Emets, "Electric Field of Insulated Wire at the Interface of Two Dielectric Media," IEEE Transactions on Dielectrics and Electrical Insulation, Vol. 4, No. 4, August 1997.

[11] "EMP Engineering and Design Principles," Bell Laboratories Report, Whippany, NJ, 1975, Chapter 2.

[12] E. F. Vance, **Coupling to Shielded Cables**, R. E. Krieger, 1987.

[13] K. S. H. Lee (editor), **EMP Interaction: Principles, Techniques, and Reference Data**, New York: Hemisphere Publishing Co., 1986, pp. 376-391.

[14] F. M. Tesche, M. V. Ianoz, and T. Karlsson, **EMC Analysis Methods and Computational Models**, New York: John Wiley & Sons, Inc., 1997.

[15] C. E. Baum, "Effect of Corona on the Response of Infinite-Length Transmission Lines to Incident Plane Waves," AFWL Interaction Note 443, February 6, 1985.

[16] J. P. Blanchard, "A Calculational Model of Corona Effects on a Conducting Wire in a High Altitude Electromagnetic Pulse (HEMP) Environment," AFWL Interaction Note 455, November 21, 1985.

[17] I. S. Gradshteyn and I. M. Ryzhik, **Table of Integrals, Series, and Products**, New York, Academic Press, 1965,p. 366.

[18] F. M. Tesche, "Comparison of the Transmission Line and Scattering Models for Computing the HEMP Response of Overhead Cables, IEEE Transactions on Electromagnetic Compatibility, Vol. 34, No. 2, May 1992.

[19] P. Degauque, G. Courbet, and M. Heddebaut, "Propagation Along a Line Parallel to the Ground

Surface: Comparison Between the Exact Solution and the Quasi-TEM Approximation," IEEE Transactions on Electromagnetic Compatibility, Vol. EMC-25, No. 4, Nov. 1983.

[20] E. C. Jordan and K. G. Balmain, **Electromagnetic Waves and Radiating Systems**, Englewood Cliffs, New Jersey: Prentice-Hall, Inc., 1968, pp. 146-147.

[21] L. K. Warne and K. C. Chen, "A Bound on Aperture Coupling from Realistic EMP," IEEE Transactions on Electromagnetic Compatibility, Vol. 36, No. 2, May 1994.

[22] M. Abramowitz and I. A. Stegun (editors), **Handbook of Mathematical Functions**, Washington, DC: National Bureau of Standards, pp. 298,1027.

[23] Y. L. Luke, **The Special Functions and Their Approximations**, Volume 2, New York: Academic Press, 1969, p. 195.

[24] K. C. Chen and L. K. Warne, "Improved asymptotic expansions of time domain antenna current," Radio Science, Vol. 26, No. 5, pp. 1205-1208, Sept.-Oct. 1991.

[25] Y. L. Luke, **Mathematical Functions and their Approximations**, New York: Academic Press, 1975, pp. 119-138.

Distribution:

1 Dr. Mike Frankel
IDA/EMP Commission
4850 Mark Center Drive
Alexandria, VA 22310

1 Dr. C. E. Baum
AFRL/DEHP Bldg 909
3550 Aberdeen Avenue S.E.
Kirtland AFB, NM 87117-5776

1 ITT Industries/AES
Attn: K. S. H. Lee
1033 Gayley Avenue
Suite 215
Los Angeles, CA 90024

1	MS1152	W. A. Johnson, 01642
1	MS1152	R. E. Jorgenson, 01642
10	MS1152	L. K. Warne, 01642
1	MS1152	M. L. Kiefer, 01642
1	MS1152	L. X. Schneider, 01643
2	MS1152	M. E. Morris, 01642
1	MS1152	M. Caldwell, 01643
1	MS1152	M. A. Dinallo, 01643
5	MS0405	W. J. Tedeschi, 05923
1	MS0405	T. R. Jones, 12333
1	MS0405	Y. T. Lin, 12333
1	MS0405	K. O. Merewether, 12333
10	MS0492	K. C. Chen, 12332
1	MS9018	Central Technical Files, 8945-1
2	MS0899	Technical Library, 09616